Hindawi
Shock and Vibration
Volume 2021, Article ID 8821986, 27 pages
https://doi.org/10.1155/2021/8821986

Review Article

A Review of the Research and Development of High-Frequency Measurement Technologies Used for Nonlinear Dynamics of Drillstring

Lixin Li,[1,2] Jin Wang,[3,4] Yingmei Yu,[5] Yifei Xing,[1,2] Fengyan Zhang,[1,2] Yi Zhang,[1,2] and Yanyan Li[1,2]

[1]*Chinese Academy of Geological Sciences, Beijing 100037, China*
[2]*China Deep Exploration Center, China Geological Survey, Chinese Academy of Geological Sciences, Beijing 100037, China*
[3]*School of Engineering and Technology, China University of Geosciences, Beijing 100083, China*
[4]*Key Laboratory of Deep Geodrilling Technology, Ministry of Land and Resources, Beijing 100083, China*
[5]*Shijiazhuang Senior Technical School, Shijiazhuang 050040, China*

Correspondence should be addressed to Jin Wang; wjzym286@163.com

Received 27 August 2020; Revised 20 November 2020; Accepted 11 June 2021; Published 28 June 2021

Academic Editor: Marco Alfano

High-frequency measurements can provide much more new insights for drillstring dynamics compared to traditional instruments, leading to a new realm of understanding of drillstring behaviors in great detail than before. In this paper, data acquisition tools with high-frequency sample rates and the data processing are introduced. Based on high-frequency data, progress of drilling dynamics is summarized, including new understandings of low-frequency drillstring dynamics, high-frequency torsional oscillations (HFTOs), and high-frequency axial oscillations (HFAOs) and new findings for the coupling of vibrations and motions, as well as models and simulation methods to deeply comprehend high-frequency dynamics of drillstring. High-frequency measurements have been used for enabling drillers to improve drill performance, especially for field decision making, BHA selection, and bit design, usually through the ways of minimizing vibrations to obtain high-efficient drilling conditions, the high-frequency response near bit can also be used for lithology identification during drilling. Though there still exists a gap between research perspective and drilling practice, the industry of high-frequency measurements has gotten off a good start, which has huge potential to avoid nonproductive time thereupon reducing drilling cost in the future.

1. Preface

Nonlinear systems, characterized by nonregularity, nonadditivity, and unpredictability, widely exist in drilling process, particularly in dynamics of drillstring. In these systems, nonlinearity arises from the large, coupled deflection that occurs in the downhole components as they move around within a long and narrow borehole, and the frictional contact that results from the borehole wall restraining that movement [1]. With a huge length-diameter ratio, the drillstring possesses complicated dynamics under the complex stress situations and multidimensional vibrations during its rotational motion, typical vibration behaviors, such as longitudinal vibration, transverse vibration, torsional vibration (stick-slip), and whirling, are coupled in varying degrees and closely related to drilling safety and efficiency. Under the shock and vibration of drillstring, fatigue failure of drillstring, excessive wear of bit, instability of wellbore, and damage of downhole tools might be occurred, which lead to drill accidents that even result in borehole abandonment. According to statistical results, operational failures related to shock and vibration generated hundreds of millions of dollars in loss, representing more than one-quarter of the total loss reported and 25% nonproductive time (NPT) [2–7]. For effectively optimizing drilling efficiency, reducing the cost and risk while obtaining

considerable impact and benefits, the drillstring dynamics must be taken into consideration. Proper modeling and monitoring is essential to prevent drillstring dynamics from causing severe drilling problems [3, 8].

Since Lubinski [9] put forward the secondary bending theory in 1950, drillstring dynamics has been one of the most important and attractive research fields in the oil and gas industry for the last 70 years or so. Moreover, model evaluation and experiment have been used to revealing the root causes, vibration control technologies, and applications. The phenomena, such as inherent frequency of drillstring, drillstring precession, coupling of different vibrations and whirl, chaos behavior of bottom-hole assembly (BHA) motion, and the relationship between bit and formations, are confirmed and discussed in detail [2, 10–16]. It has been proved that there is a close connection between the drillstring dynamics and drilling parameters and the seemingly irregular behaviors with random characteristics have somewhat nonperiodic ordering. However, the surface measurements were found to be inconclusive with respect to downhole behaviors [17]. For deeply understanding the intrinsic nature of the out-of-order behavior of this nonlinear systems, downhole measurements were started to support the drillstring dynamic research in the 1990s. After that, the research of drillstring dynamic stepped into the rapid development stage, and the vibrations and their correlation with formation characteristics, BHA whirl and bit bounce, resonance of the BHA, and vibration control and mitigation were researched based on downhole data [18–23], effectively promoted the BHA design and the production increasing.

Traditionally, sensors with low sample frequency were used to collect downhole data, but researchers gradually verified that sample at low frequency was inadequate, and the data quality starts to limit the performance of dynamic research [24]. High-frequency data with more information are urgent need for drillstring dynamic research. Analysis of high-frequency data appears to be particularly useful to better characterize and understand vibration events, which are prominent technical limiters of drilling performance [25]. Actually, high-frequency measurements with sampled at hundreds or thousands of Hz have been widely used in the oil and gas industry for estimating the solid particle content in extraction fluid [26], monitoring rig vibrations and shaker condition [27, 28], and anticollision monitoring of casing [29]. However, for the reason of more challenging of design and calibration of downhole sensors than that on surface, the application of high-frequency measurement used for downhole dynamics is lagging behind, and the usage of high-frequency data is still a frontier to drillstring dynamic research studies.

In recent years, downhole dynamic data collected at increasingly high sample rates provide new insights and evidences for downhole motions and forces, improved our understanding of the dynamic behavior of the bit, BHA, and drillstring. The high-frequency data include vibrations, bending, pressure, temperature, and rotational speed and might be used to thoroughly comprehend the drillstring dynamics, which is critical to drilling performance. In this paper, the measurement tools with high-frequency sample rates are summarized, the findings based on high-frequency dynamic data, such as whirl, high-frequency torsional oscillation (HFTO), the coupling of high-frequency vibrations, and low-frequency stick-slip are reviewed, some applications or potential applications using high-frequency techniques are introduced, and then the expectation and advices of high-frequency drillstring dynamics are given.

2. High-Frequency Data Acquisition for Drillstring Dynamics

Traditional vibration or shock detecting is based on measurement while drilling (MWD) devices and surface monitor instruments, by which the phenomenon with low frequency, such as stick-slip, and transverse or longitudinal vibrations, whirl, are observed. Dong and Chen summarized the different forms of vibrations and shocks and its dominant characteristics [30], as shown in Table 1. Most of the three basic modes of drillstring, such as axial (longitudinal) mode, torsional (rotation) mode, and transverse (lateral) mode, own a relatively low frequency below 50 Hz. Simultaneously, some of the vibrations of drillstring own distinct high-frequency characteristics, the frequencies magnitude of torsional resonance and bit chatter are up to hundreds of Hz, and the maximum frequency and amplitude of torsional resonance can reach to about 560 Hz and 200 g [31]. According to the Nyquist–Shannon theorem [32], the sampling rate should generally be at least twice as high as the highest frequency of interest, the sample rate of drillstring dynamic research studies must be reached to hundreds of Hz in some cases, and just using low-frequency data cannot meet the requirements. The improvements in measurement capability of the drilling dynamic tools had been showed the significance of drillstring dynamics on reliability of downhole tools and overall drilling performance, advanced data acquisition tools with high sample rates are urgently needed.

2.1. Data Acquisition Tools. Different kinds of instruments that contain different kinds of sensors are developed for acquisition high-frequency dynamic parameters of one-axis or triaxial accelerators, RPM, bending moment, weight on bit, torque, and so on. Measurements for drillstring dynamics with high-frequency sample rates are listed in Table 2, respectively, which can be mounted on surface rig, or at the bottom, or along the drillstring for multiple purposes, which is very helpful for better understanding the high-frequency dynamics of drillstring and optimizing the system performance. The sample ability of these tools ranges from 50 to 5020 Hz, in which the modular device has the highest sample rate during experiment testing. In these tools, ISS is a special kind of drillstring dynamic measurement tool mounted on surface, the sample rate ranges from 50 to 500 Hz, and the data are transmitted by wireless signal. Due to the surface measurement cannot precisely identify the occurrence of downhole vibrations, the majority tools are designed to install on BHA or along the drillstring to collect data in real time to improve our understanding of the dynamic behavior of the bit, BHA, and drillstring. The information obtained in high-frequency data has provided significant insight into the response of the drilling system to

Table 1: Classification and comparison of drill string vibration and shock [30].

Forms	Mode of vibration			Frequency (Hz)	Amplitude (g)	Tool damage
	Axial/longitudinal	Transverse/lateral	Torsional/rotational			
Stick-slip	—	—	√	0.1~5	0~10	PDC cutter damaged, drill string twist off or washout
Bit-bounce	√	—	—	1~10	0~100	Bit damaged and BHA washout
Bit whirl	—	√	√	10~50	0~200	Cutter and/or stabilizers, increased torque
BHA whirl	—	√	√	5~20	0~100	Cutter and/or stabilizers, increased torque
Lateral shock	—	√	—	1~5	0~14	BHA washout
Torsional resonance [31]	—	—	√	20~500	—	Cutter and/or stabilizers, increased torque
Parametric resonance	√	√	—	0.1~10	—	Cutter and/or stabilizers, increased torque
Bit chatter	—	√	√	20~250	—	Bit damaged and BHA washout
Vortex-induced vibration	—	√	—	0.1~20	—	Riser damage
Modal coupling	√	√	√	0.1~350	—	Drill string twist off/ washout

Comments: according to Hohl's opinion [31], the frequency of torsional resonance (such as HFTO) could reach to 500 Hz, which is different from Dong and Chen [30].

initiating rotation; drilling procedures and parameter modifications; and exposure to excitation from sources including, but not limited to, rig heave, BHA component imbalance, and bit-rock interaction [51].

Limited by transfer rates of mud pulse telemetry (typically 20 bits/seconds by advanced shear valve pulser [52]), the downhole data acquisition usually used networked drillstring telemetry and downhole storage (memory mode). High sample rate tools can be traced to Wire Telemetry System (WTS) by NL Industries Inc. In 1985 [18], the sample rate was 650 Hz and the downhole data were transmitted to surface based on wired drillstring technology. The wireline system provides a two-way communication link between downhole sensors and surface, the downhole electronics can be powered from the surface, and the wireline can be quickly extracted from the drill string for any required maintenance or repair [53]. By using wired drillpipe technologies, the transfer rates of networked drillstring telemetry can reach to 57600 bits/seconds (equivalent to 1800 32-bit numbers per second) with real-time bidirectional broadband communication between surface and downhole, by which new possibilities with regard to downhole dynamic monitoring are opened [54] and downhole dynamic tools such as DWD and BlackStream Series are developed. Compared to networked drillstring telemetry, data collected by downhole storage mode are unlimited by transfer rate, and the vibration signals can be stored in memory disk when sensors get the data. After tripping-out the drillstring, the storage data can be read by playback in post-run analysis to perform detailed investigations. Generally, the largest amount of downhole tools with high sample rates is based on memory mode, such as DDMT, Security DBS, TVM, DMM, DDR, and BlackBox [55].

Some advanced drillstring dynamic measurement tools are shown in Figure 1. Most of the downhole tools, such as DWD, DMM, and BlackStream Series, are made as downhole sub, and the structure of DWD measurement tool and BlackStream ASM tool is shown in Figure 2, respectively, represented the design scheme based on downhole memory mode and wired drillstring transmission mode. Specially, the DDR tool and its updated version BlackBox Eclipse II, as well as the CuBic Puk, are made as button-like shape and can be mounted on anywhere of the drillstring with a customized carrier box. The work temperature and pressure of majority tools in Table 2 can, respectively, reach to 150°C and 20000 psi, the TVM owns the best performance for high temperature and high pressure, and the work temperature and pressure can reach to 180°C and 30000 psi, by which downhole data in deep well drilling can be acquired. The advanced tool such as vibration MWD tool is a well-established industry standard MWD tool (with up to 1000 Hz at a sampling rate of 2500 Hz, 200 g sensors for each axis, 4 GB memory) for downhole dynamics and drilling optimization, and it is located above the rotary steerable system and owns the ability of transferring averaged data to surface in real-time and storing raw data in memory for post-well analysis. The recent increase in vibration measurement bandwidth up to 1, 000 Hz has increased the acceleration sensor range to 200 g [56].

2.2. Downhole Processing of High-Frequency Data. To realize effective monitoring while drilling, some of downhole storage dynamic measurement tools possess the function of in situ data processing, and the raw data stream from sensors sampled at high frequency can be converted into low-frequency (normally 0.2–0.5 Hz) statistic values, such as average, minimum, maximum, root mean square (RMS), and root mean cube (RMC) values. These data with relatively low

Table 2: Measuring instruments for dynamic drillstring with high-frequency sample rates.

Time	Equipment	Author or inventors	Installation location	Sample rates (Hz)	Measuring parameters									Data acquisition style
					WOB	TOR	BM	RPM	ACC	TEM	HL	AP	IP	
1985	Wire Telemetry System (WTS) [18]	NL Industries Inc.	BHA	650	√	√	√	√	√	√	√	√	√	Wired drillstring
1993	Drillstring dynamic sensor (DDS) [17, 33]	Amoco Co. & Halliburton	BHA	500–2000	√	√	√	—	√	—	—	√	—	Downhole storage
1998	MWD downhole recorder [34]	Baker Hughes	BHA	1000	√	√	√	—	√	√	—	√	—	Downhole storage
2003	Diagnostic while drilling (DWD) [35]	Sandia National Laboratories	BHA/ drillstring	60–2080	√	√	√	√	√	√	—	√	√	Wired drillstring
2004	Security DBS [36]	Halliburton	BHA	2000	√	√	—	—	√	√	—	√	—	Downhole storage
2008	True-vibration monitor (TVM) [37]	Weatherford	BHA	1000	√	—	—	√	√	—	—	—	—	Downhole storage
2011	Instrumented saver sub (ISS) [38]	Bill Lesso et al.	Surface	50–500	—	√	—	√	√	√	√	—	√	Wireless transmission
2011	Drilling mechanics module sub (DMM) [38]	Bill Lesso et al.	BHA	200–2000	√	√	√	√	√	√	—	√	√	Downhole storage
2012	Downhole dynamic recorder (DDR) [39, 40]	National Oilwell Varco	BHA/ drillstring	400	√	√	√	√	√	√	—	√	√	Downhole storage
2012	Modular device (MD) [41, 42]	Baker Hughes	BHA	500–5120	√	—	—	√	√	√	—	—	—	Downhole storage
2014	Drilling dynamic measurement module (DDMM) [43, 44]	Schlumberger	BHA/ drillstring	2048	—	—	—	√	√	√	—	—	—	Downhole storage
2017	BlackStream Tool Series [45–47]	National Oilwell Varco	BHA/ drillstring	80–800	(√)	(√)	(√)	√	√	√	—	√	√	Wired drillstring
2019	CuBIC HF [48]	Turbo Drill Industries, Inc.	BHA	800–1600	—	—	—	√	√	√	—	—	—	Downhole storage
2019	Downhole vibration measurement tool (DVMT) [49]	Sinopec	BHA	1000	—	—	—	√	√	—	—	—	—	Downhole storage
2019	BlackBox Eclipse II [50]	National Oilwell Varco	BHA/ drillstring	800–1500	—	—	—	√	√	√	—	—	—	Downhole storage

Comments: WOB, TOR, BM, RPM, ACC, TEM, HL, AP, and IP, respectively, refer to weight on bit, torque, bending moment, revolutions per minute, acceleration, temperature, hook load, annular pressure, and internal pressure.

frequency can be transmitted by mud pulse to surface by instruments such as MWD downhole recorder and TVM when they are installed as a part of MWD or complemented with a MWD.

In general, the high-frequency data are memorized in downhole tools whatever the wired drillpipes or MWD is used. Data storage capacities for downhole measuring are limited by the design of drilling tools, and manufacturers have traditionally applied different approaches, collecting both "burst data" and "continuous data." Burst data are a kind of high-frequency snapshot sequences for the analysis of downhole dysfunctions, and it can be taken at periodic time sequences or initiated though triggers last for 5 or 10 seconds. Continuous data are calculated into key statistical parameters instantly by algorithms when sample data are obtained at high-frequency rates, and then RMS, minimum, and maximum values are stored within a time window of several seconds [25]. Recently, advanced tools own the ability of recording continuous high-frequency sample data for a long durations (minutes to hours), and these data provide more information of drillstring dynamics to understand the drilling system and increase drilling performance. The workflow of high-frequency data acquisition and processing is shown in Figure 3, and the sample rate of 50 Hz

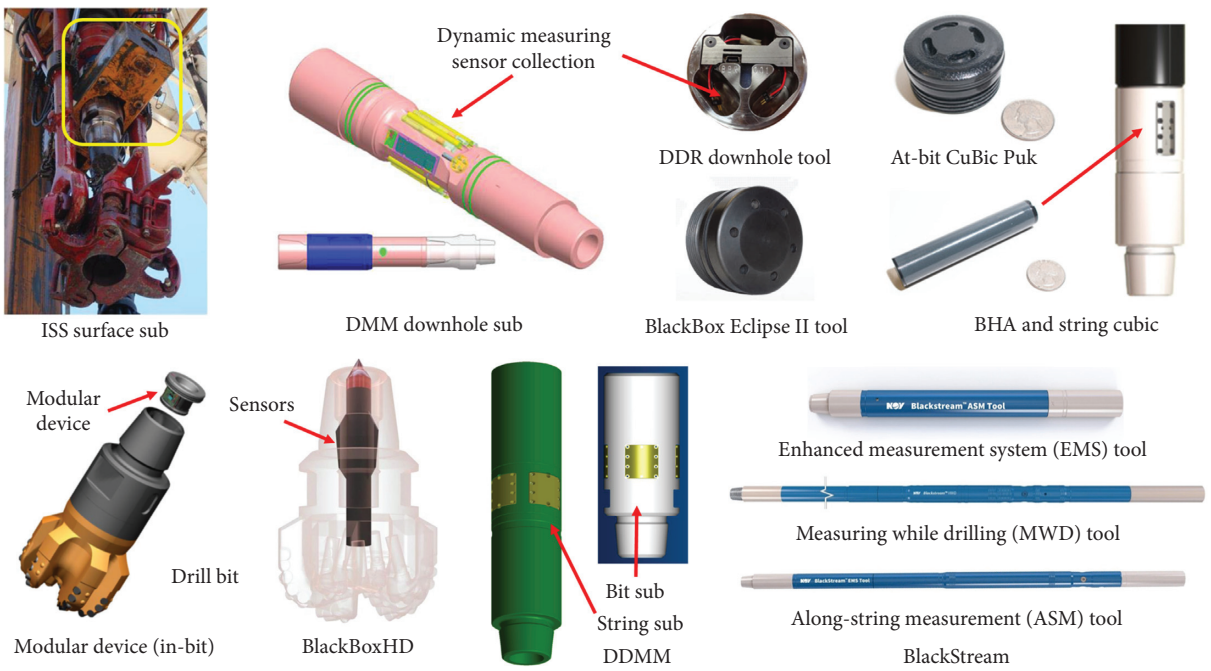

Figure 1: Some of the advanced drillstring dynamic measurement tools.

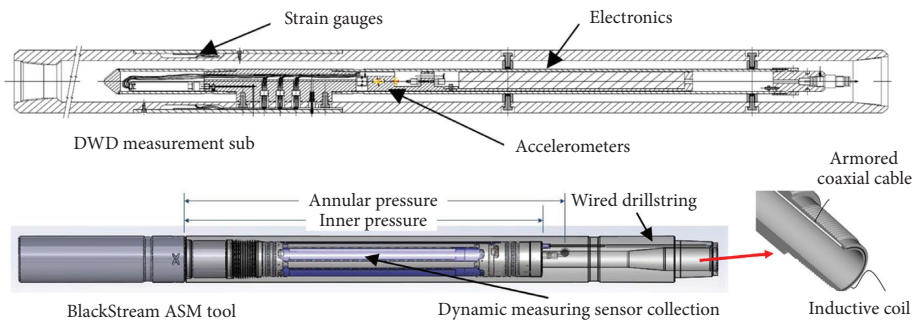

Figure 2: Structure of measurement tool based on downhole storage mode (DWD) [35] and wired drillstring transmission mode (BlackStream ASM tool) [46].

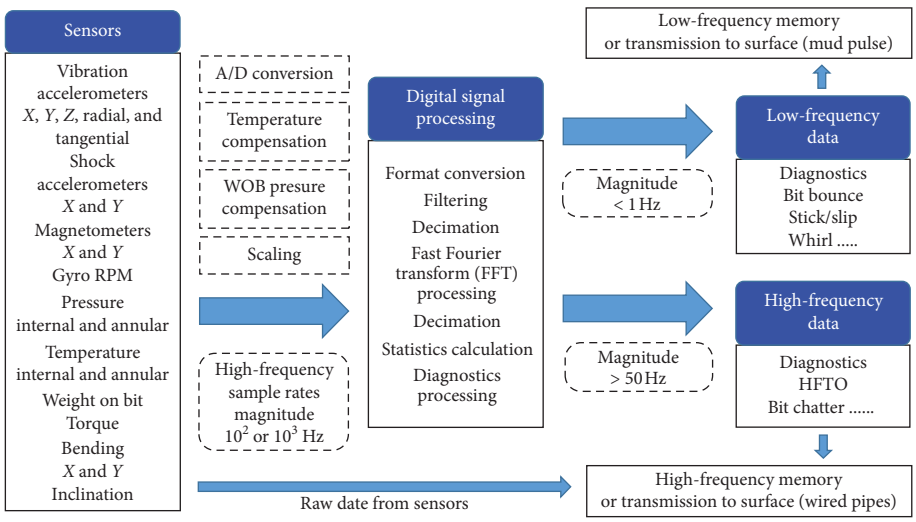

Figure 3: Data acquisition and processing block diagram.

is used as the boundary value between low and high frequencies [51].

During data processing, it should be noted that the inclination of the hole and the inclination of the recording tools themselves change during the run, and this fact needs to be taken into account while analyzing the measured accelerations. The phenomenon observed in lateral accelerometer, tangential accelerometer, and axial accelerometer data has been proven typically attributed to whirl, torsional fluctuations of drillstring and bit bounce, as shown in Figure 4, which is beneficial to downhole dysfunction diagnosing.

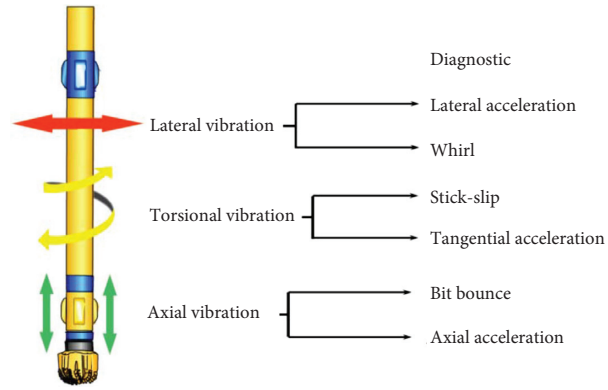

Figure 4: Modes of vibration and its diagnostic [57].

3. Progress of Drillstring Dynamics Based on High-Frequency Data

Through using measurement tools with high-frequency sample rates mentioned above, data with more information provide us new insight and evidence for drillstring dynamics. The high-frequency measurements are used to verify vibration propagation distance/pattern and frequency response. The data measured provided critical information to understand tool response characteristics under different drilling parameters, inclinations, and conditions. By these data, better understanding of basic vibration modes is obtained, some new phenomena such as HFAO and HFTO are discovered, and the studies of complex coupling between different oscillations of drillstring have made a great progress.

3.1. New Understandings of Drillstring Dynamic Behaviors with Low Frequencies

3.1.1. Lateral and Longitudinal Vibrations. A wide range of vibrations has been captured in which the drilling system switched from a dominant vibration mode, typically torsional (downhole rotation-velocity oscillations or stick/slip) into a different mode, such as axial (bit bounce) or lateral (whirl). By using two modular devices, respectively, mounted on bit and BHA (15m above the bit), Hoffmann et al. [42] compared the lateral vibration data and found that low-frequency vibrations were higher in the BHA while the high-frequency vibrations were higher at the bit over the entire run, confirmed that the low-frequency vibrations were BHA-induced and the high-frequency vibrations were bit-induced. The overall vibrations in both locations are dominated by the high-frequency vibrations, by which suggested that the bit-induced vibrations could propagate into BHA and may lead to BHA failures.

The effects of poor tool face control and weight transfer accumulate over the length of the well, compounding the problem as the well gets deeper. This leads to high torque and drag which ultimately reduces drilling performance, even in rotary mode. To solve this problem, the use of friction reduction tools (FRTs) with steerable motors has become common place in North America. Downhole instrumented sensors with high-frequency sample rate were used to confirm the value of the FRTs. The application effect of axial oscillation tool (AOT) and lateral vibration tools (LVTs) was evaluated by Gee et al. [58] with five high-frequency measurement devices included in the drillstring in a tangent well drilled in the Middle East. The axial vibrations generated by the AOT (approximately at 18 Hz) can be measured over several hundred feet or as much as over a thousand feet away from the tool was verified (as shown in Figure 5), and AOTs can provide more effective drag reduction and significantly improve more drilling performance compared to LVTs in similar offset wells according to field cases. The effect of AOT and its placement optimization were also evaluated by Shor et al. through simulation and field [59]. The analysis of in situ burst data acquired by DDRs showed that acceleration magnitude with an AOT is overall somewhat higher than that experienced in the BHA without an AOT, and a shock sub should be installed below the AOT to obtain a greater portion of the oscillation energy directed upward. This may be beneficial for AOT applications with long laterals due to the friction reduction desired to improve WOB transfer. Both VOTs and LATs could have negative impact on reliability of electronic and mud pulse equipment results in nonproductive time tripping for failed equipment due to the fact that oscillations and vibrations are being introduced to the BHA and drill string. A new axial FRT was developed by Jones et al. [60], and the high-frequency burst data showed that no excessive shock and vibration were being induced into the BHA and string from the FRT, presented that the FRT was effective in transmitting axial oscillations along the BHA without introducing any damaging effects to the BHA.

3.1.2. New Insights of Backward Whirl. The measurements from the downhole sub provide a clearer understanding of the loading placed on downhole equipment by backwards and chaotic whirl motions. This information is useful for predicting the life of downhole components and developing measures to avoid downhole failures such as tool design and schedules for inspection and maintenance of downhole tools.

According to high-frequency data conducted at directional drilling test facility, Lesso et al. [38] classified four typical behaviors of drillstring state, as shown in Figure 6. In Figure 6(a), the drillstring is not subject to extensive bending

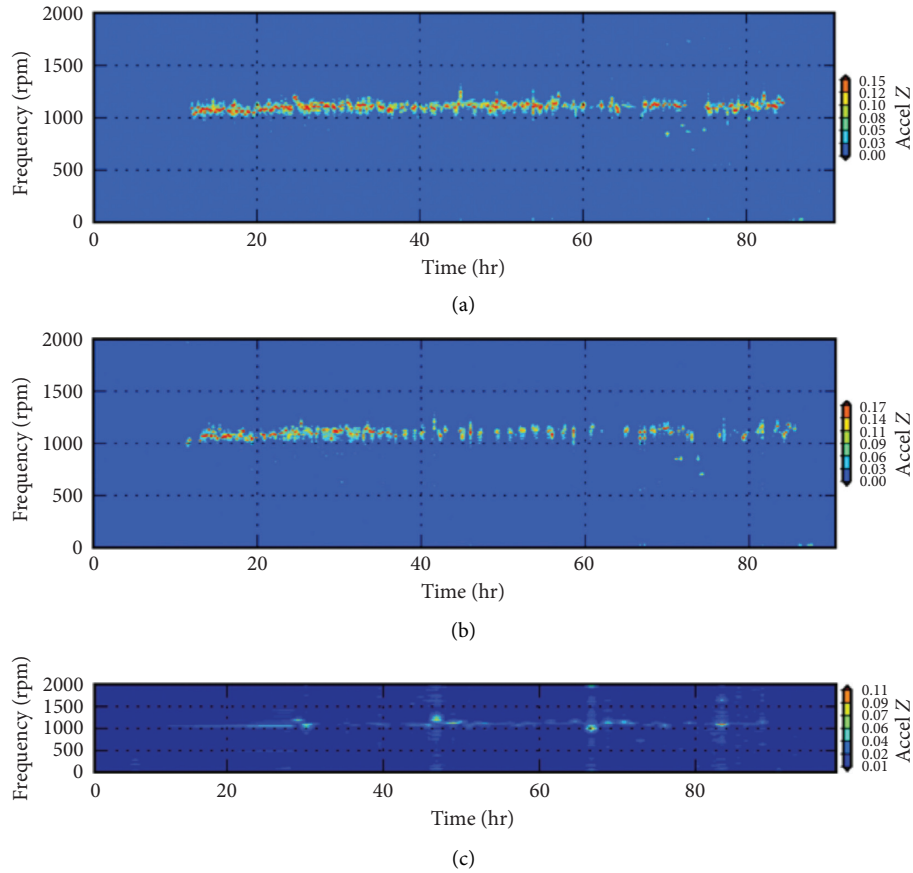

Figure 5: Burst frequency signal at different positions of drillstring [58]. (a) Directly above AOT, 1322 ft from bit; (b) 400 ft below AOT; (c) at the bit.

or torque fluctuations during normal drilling, and the bending frequency spectrum showed that there is no dominant frequency. In Figure 6(b), the stick-slip is characterized by enormous speed fluctuations of rotation and rotational accelerations, and the drillstring can reached up to 300 rpm and then dropped to zero, with a 2-3 Hz slip RPM (red) in bending frequency spectrum. During backward whirl, a bending rate dominant frequency at 30 Hz was emergence while the drillstring RPM is 1.45 Hz (105 rpm), as shown in Figure 6(c). In Figure 6(d), one of the most destructive events was captured and showed the state of coupled stick-slip with backward whirl engaging on the slip phase, and the bending in the slip interval shoots directly to a high frequency approaching 50 Hz.

By using downhole high-frequency field data during underreaming vertical well with a BHA including 18.125-in. PDC bit, push-the-bit rotary steerable system (RSS), and 21-in. underreamer, Bowler et al. [51] discussed different vibration types of whirl in detail. As shown in Figure 7, the forward whirl (blue lines) and backward whirls (red lines) are both measured, and a transition to chaotic whirl triggered by borehole contact was depicted; the high-frequency data whirl cross-plots of the bending due to whirl at 04:32:15 (a), 04:32:30 (b), 04:32:45 (c), and 04:33:00 (d) are, respectively, characterized as the transition into forward whirl, the state of forward whirl, the transition into chaotic whirl, and the state of chaotic whirl. During this period, the surface parameters (ROP and RPM) were constant, and the main drivers for chaotic whirl are thought to be lateral excitation and high friction at contact points between the BHA and the wellbore. Chaotic whirl creates high shock and large fluctuations in bending moment, which can lead to high risk of BHA and rapidly damage downhole components, especially those containing electronics. Additionally, the downhole high-frequency sensors were able to characterize the off-bottom instability of the system during drillstring connections and were able to refine procedures. During back-reaming in a directional well with inclination of 50° using a large-hole-size underreaming-while-drilling assembly, the transitions from low-severity backward whirl into fully developed high-severity backward whirl are observed (see Figure 8). It indicates that the location of stabilizers below underreamer must be considered to prevent downhole failures.

Based on field data sampled at high frequency, a backward whirl at around 57 Hz was observed by Oueslati et al. [24], and then the reason of backward whirl was illustrated. As shown in Figure 9, the blue arrows and red arrows, respectively, represent the cutting direction and the bit velocity, the instant center of rotation of the bit is the contact point between the bit and borehole wall without slippage, the velocity profile of the bit is depicted along three

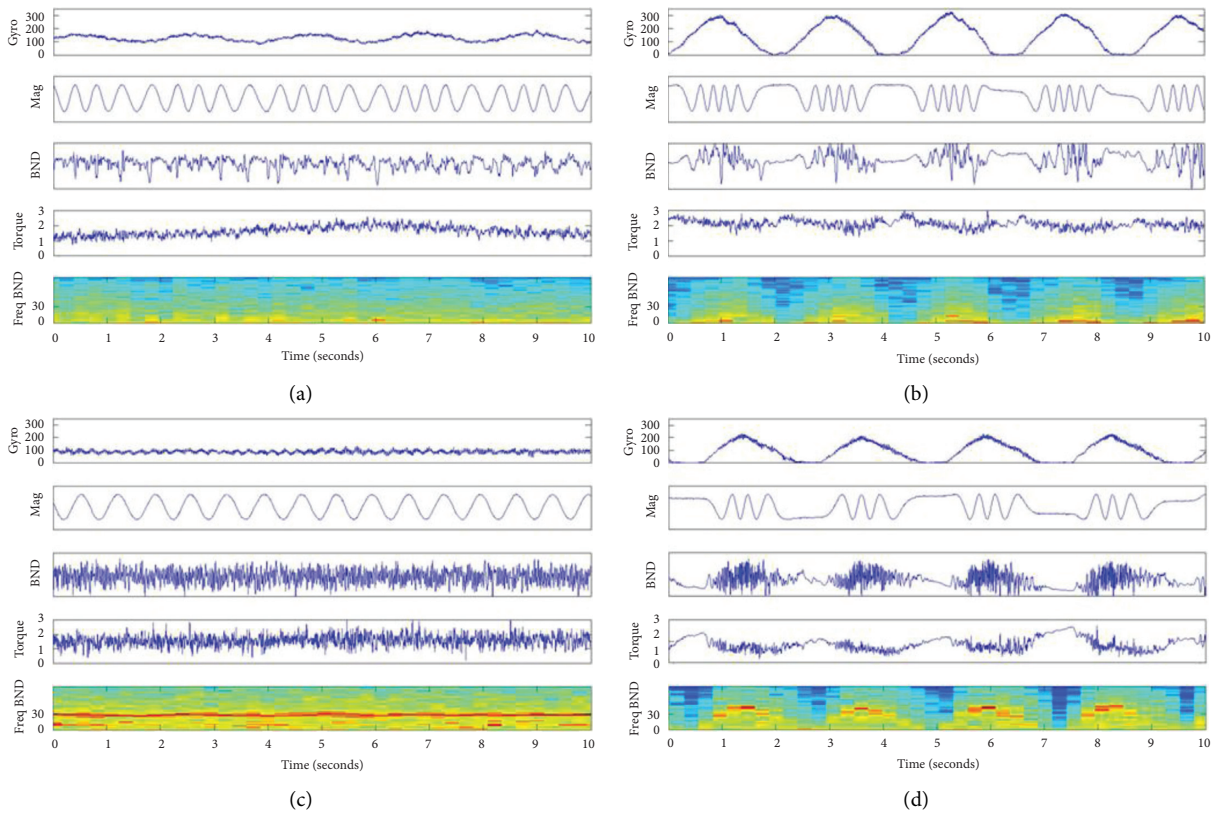

Figure 6: High-frequency data acquired during (a) normal drilling; (b) stick-slip while drilling; (c) backward whirl while drilling; and (d) backward whirl with stick-slip [38]. Five tracks from up to down, respectively, are rate gyro (RPM), magnetometer, bending moment, torque, and bending frequency spectrum (Hz).

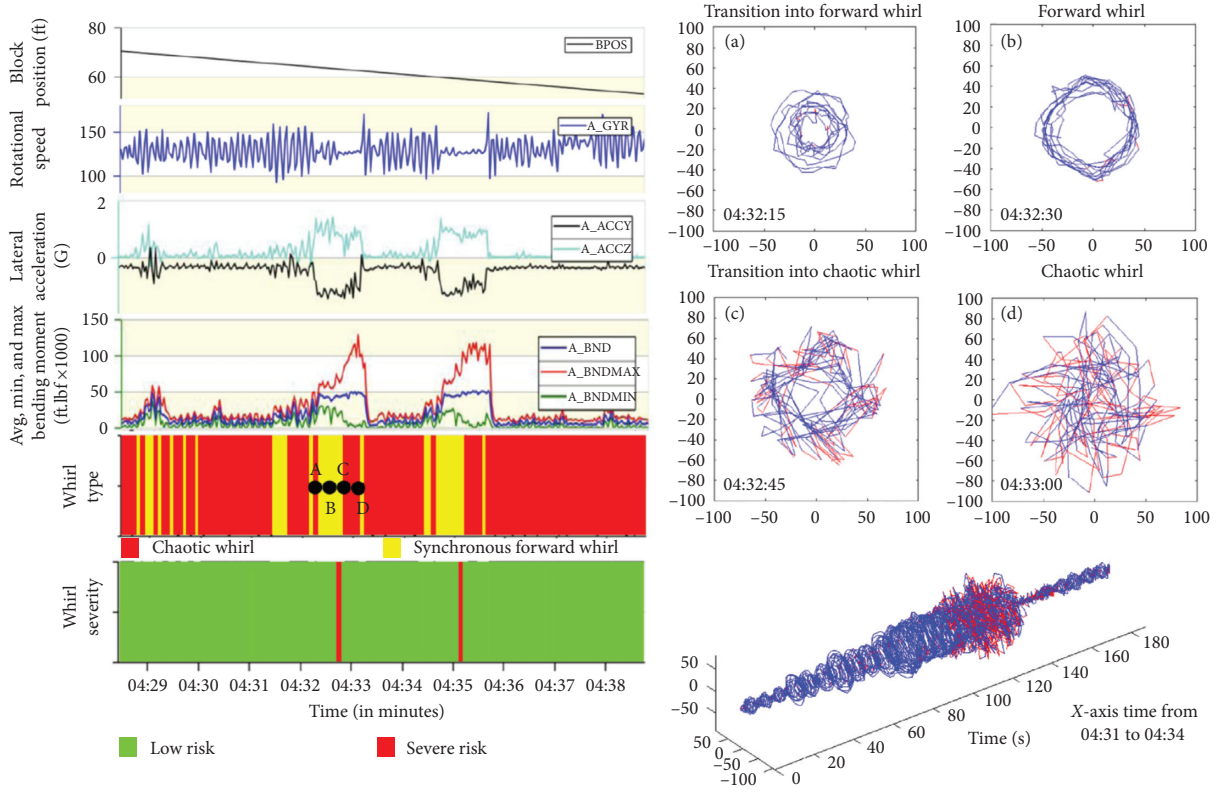

Figure 7: Transition from forward whirl into chaotic whirl [51]. Bending moment (ft. lbf × 1000) is measured in two directions (Y and Z) and cross-plotted using tool face to allow a visualization of the lateral motion of the downhole sub collar.

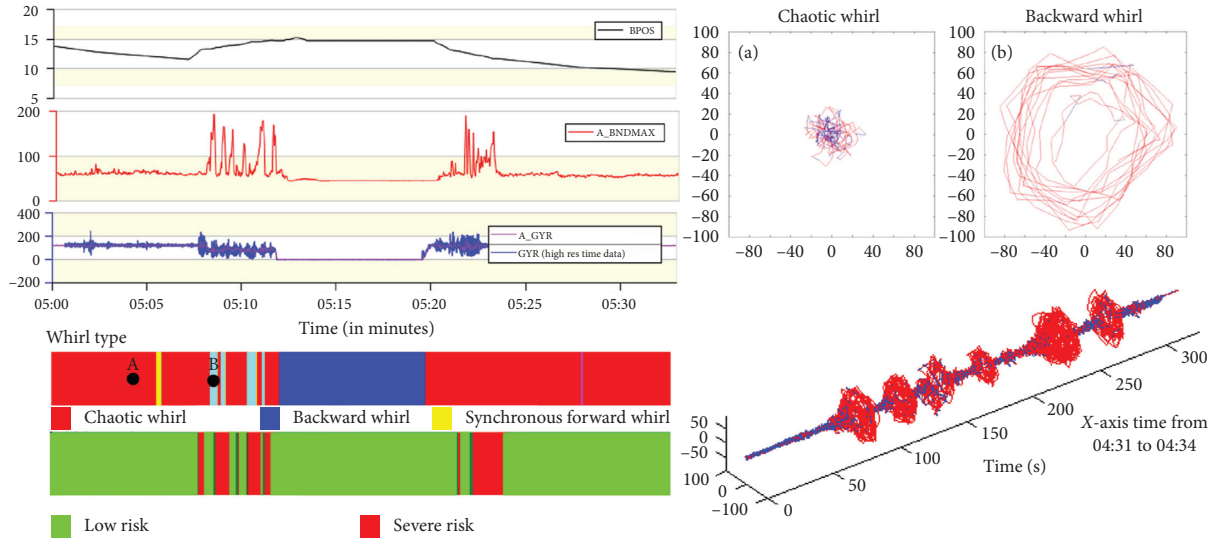

Figure 8: Transition from stable to unstable when picking up off-bottom with rotation [51].

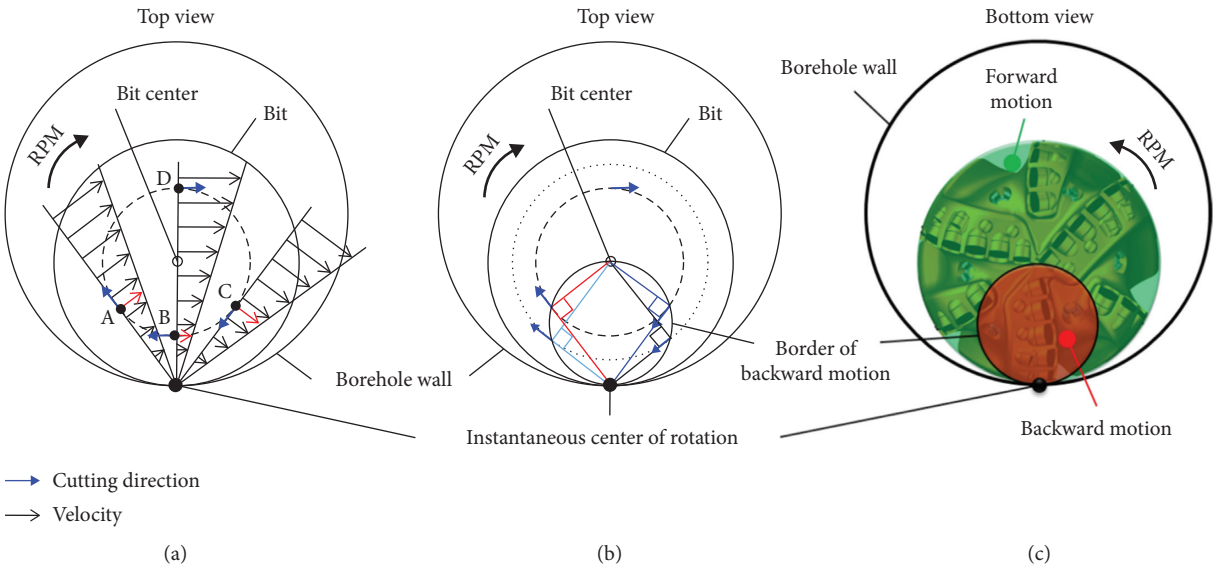

Figure 9: (a) Velocity profiles of the bit in the borehole along three exemplary lines. (b) Border of backward rotation with Thales' theorem. (c) Bottom view of the bit and areas of backward and forward motion [24].

exemplary lines, and the dotted circle demonstrates on trajectory of cutters. At points A and C, the cutting direction and cutter velocity are orthogonal to each other and the cutter is moving sideways. On a line between the instant center of rotation of the bit and the bit center, the cutter point in the opposite direction of the velocity at point B, the nearby area (red area), is subjected to backward motion. On the other side at point D, the cutter point in the same direction of the velocity, the nearby area, is not subjected to backward motion. The border between backward and forward motion of cutters on the dotted circle is defined by points A and C, using all circles around the center of the bit, and the backward motion profile is calculated as a circle, which is defined by the instantaneous center of rotation and the bit center. The angle between the cutter direction and the velocity vector can be obtained from the inner product of both vectors to calculate the velocity in the cutter-fixed coordinate system, and the results are shown in Figure 10, in which negative values indicate backward rotation.

Based on high-frequency data, the value of vibration patterns is explored. A simple, purely kinematic model was built by Baumgartner and van Oort [25] and could be able to closely reproduce whirl vibration patterns observed in field data, both in time and frequency domains. The results show that the high-frequency fluctuations of tangential and radial accelerations could be attributed to a whirling motion of the drillstring, and the frequency of these fluctuations can reach hundreds of hertz. High-frequency snapshots of downhole accelerations show distinct patterns reoccurring throughout different bit runs, and the downhole high-frequency vibration patterns are apparently largely independent from

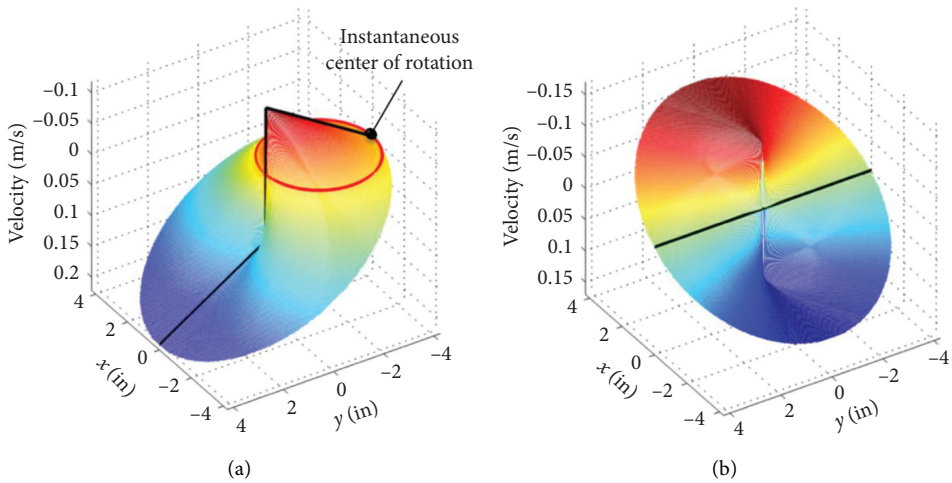

Figure 10: (a) Cutter velocity in tangential direction. The red circle corresponds to the border between backward and forward rotation, and the black line illustrates the pure tangential velocity of the cutter. (b) Cutter velocity in the sideways direction [24].

specific operational parameters as well as borehole geometry. These patterns appear to be more useful to classify and quantify vibration than absolute vibration parameter value, a methodology for automated classification of vibration from high-frequency downhole data was developed, and it correctly identified 90% of the stick-slip instances and 92% of the whirl instances, by which it offers a wealth of information on downhole dysfunctions that will help to better distinguish and characterize different modes of vibration for tailored mitigation techniques.

The high-frequency data are used in conjunction with a time-based dynamic simulation system to research the downhole dynamic response by Wang et al. [43], and three practical field drilling scenarios, respectively, are large downhole RPM variation, negative RPM issue, and BHA whirl coupled with stick-slip which are captured. The results show that the large downhole RPM variation at the bit was relevant to the BHA natural frequency, and the resonance was caused by bit-rock interaction resulting in the large RPM variation. The negative RPM observed in downhole data could be caused by stick-slip of the drillstring and bit. Additionally, a phenomenon of stick-slip coupled with BHA whirl was identified, and a backward whirling has a relatively low frequency of approximately 3 Hz, which is similar to the frequency in the string RPM. Actually, the frequency of bit backward whirl events could reach to around 60 Hz [24], and the backward whirl motion exposes the cutter to high forces and shocks form behind that can destroy the diamond table or complete cutter loss, as shown in Figure 11. These bit dynamic findings strongly provide support for bit design.

The findings mentioned above effectively validated the high-frequency measurements could be used to reduce the RPM variation by optimizing the bit and BHA design and operating parameters, which is benefit to reduce NPT and improve the drilling performance.

3.1.3. High-Frequency Surface Measuring. Lesso et al. [38] developed a new surface measurement ISS with 200 Hz sample rate can be located in the top drive, and the sheave dampening and friction of traditional surface instruments were eliminated. More meaningful comparisons between surface and downhole environments could be carried out by using ISS and downhole sub DMM. Both sensor packages contain useful diagnostic information, and the surface measurements appear to be more impacted by the top drive operating characteristics, while the downhole measurements reflect BHA characteristics. The torsional natural frequencies are researched by finite element analysis (FEA) and field data, and the results confirmed that there is some agreement with the natural frequencies from surface to downhole, as shown in Figure 12. These mean that the joint monitoring simultaneously both on surface and downhole might provide a new way to understand drillstring dynamics.

State-of-the-art top drives currently deployed have the ability to record rotary speed and torque at frequencies up to 200 Hz and have been used for stick-slip mitigation. According to the frequency spectra analysis of two different depth intervals of data recorded at 200 Hz, a clear evolution with depth is seen that the predominant frequency shifts towards the lower range with the depth increasing (see Figure 13). This result is unlike the data dominated by the resonances of BHA which did not evolve with the depth, claimed that the drillstring dominates the frequency response at the surface. Drillpipe resonances are dominated by its evolving length must be taken into consideration when analyzing the high-frequency data [59].

3.2. High-Frequency Torsional Oscillation (HFTO). The surface measurement system cannot identify the occurrence of HFTO downhole as the HFTO does not propagate along the string up to the surface but gets dampened in heavy weight drill pipes. Also, occurrence of HFTO in real time cannot be explained by conventional diagnostic log as the data plotted in real time with low frequency. Since high-frequency measurements used investigate BHA behavior, HFTO has become a topic gaining great attention in recent years due to the damage it causes to lower BHA components. Typical key indicators during failure investigation showing

Figure 11: Cutter damage from backward cutter rotation during backward whirl events [24].

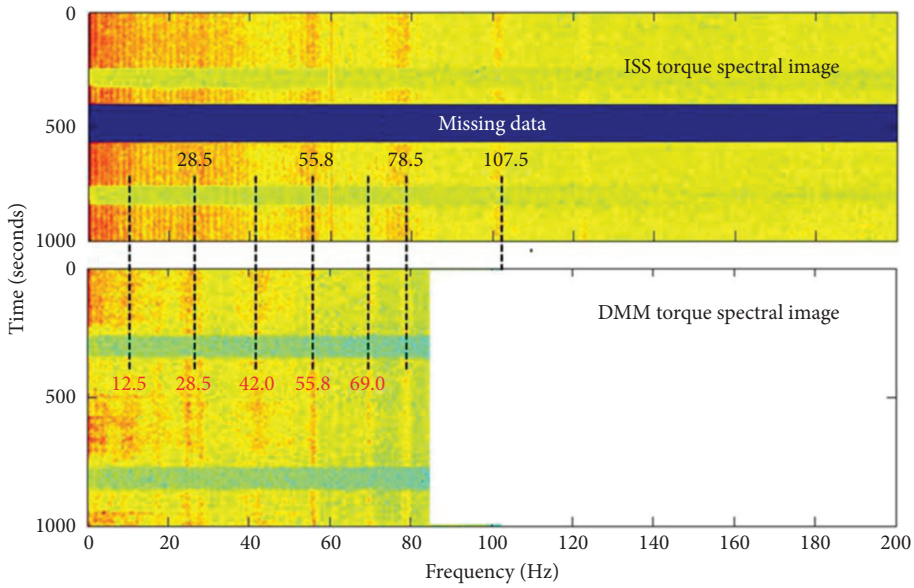

Figure 12: Spectral images from both the ISS and DMM torque measurements over about 15 minutes of drilling in rotary BHA with efficient PDC bit [38].

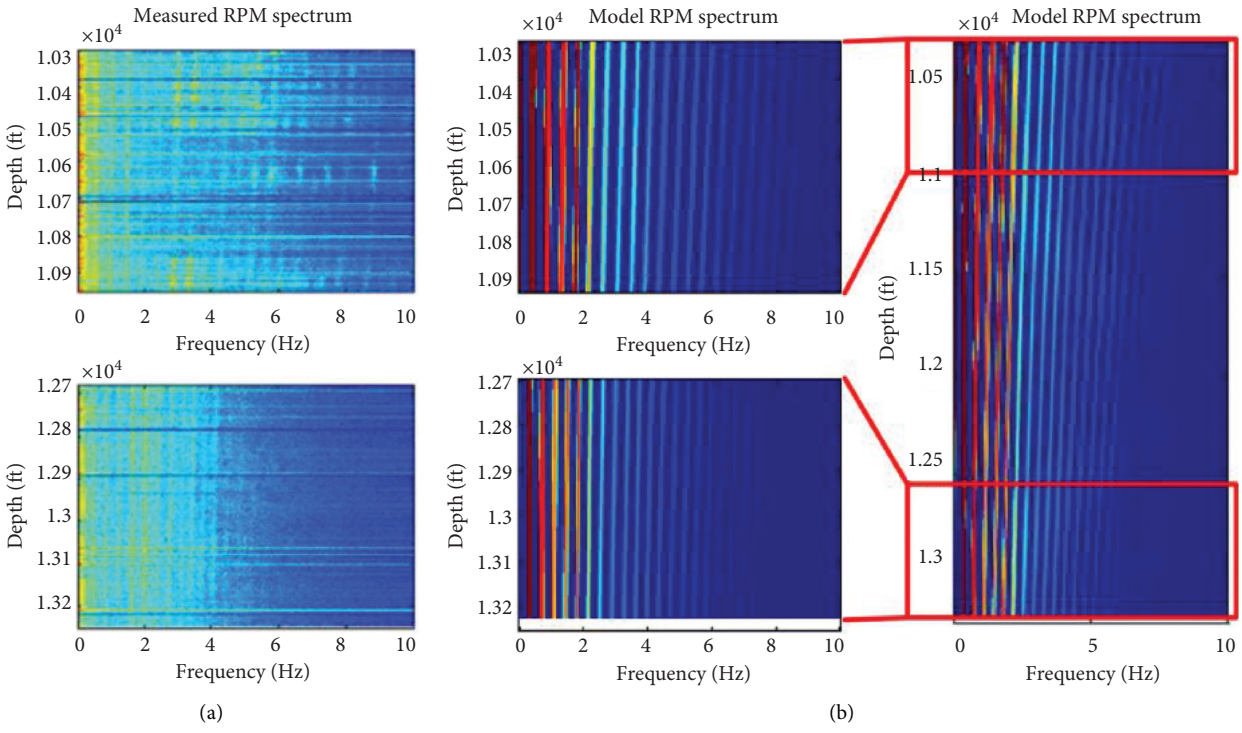

Figure 13: Surface frequency content from top drive data (a) and corresponding simulation data (b) [59].

that HFTO had occurred in a BHA while drilling are cracks on tool, loose electronics within the tool, squeezed cables, sheared bolts, and vibration dust as shown in Figure 14 [61]. Typically, the collar cracking with the crack propagating on a plane 45° from the collar axis is induced by excessive HFTO [62].

When HFTO occurs, high-frequency cyclical torque loading is introduced at each location along the BHA and drillstring. The torque amplitude at different locations depends on HFTO modes and HFTO severity. Under HFTO, the bit experiences high-frequency RPM and torque variations. The cutters experience cyclical loading which can accelerate cutter damage. Mud motor rotors and stators can undergo high-frequency torque and RPM variations, which can lead to accelerated rubber wear and tear. Since the failure of PDC cutters and the degradation of mud motor power sections have a critical effect on drilling performance, the importance of mitigating HFTO cannot be underestimated. Therefore, it is critical to investigate the root of HFTO and manage HFTO to improve drilling system life and efficiency.

3.2.1. Reasons of HFTO. HFTO, with a resonance frequency much higher than the stick-slip, is a kind of torsional instability, which is shown to be related to torsional resonant frequencies within the BHA and resulting in harmonic oscillations of the BHA. HFTO is firstly captured during drilling runs in hard formations, and then it is verified that HFTO is highly related to operating parameters and BHA, especially when using RSS. Actually, HFTO is not limited to RSS and may occur with any other BHA with or without motor in harder and denser formations all over the world [41]. Factors causing BHA to resonate in torsional direction mainly are (a) bit-rock interaction, (b) drilling parameters at the bit, (c) torsional stiffness of the BHA, (d) formation density, and (e) BHA design [61, 63].

In early time, though the torsional resonance was observed and known to result in backward rotation of bits, it is not recognized as a significant cause of PDC bit failure. Based on field downhole data, Warren and Oster [64] proposed that a wide range of PDC bits sustain the torsional resonance, which is probably the cause of rapid damage in certain hard rocks because the stress state of cutters transferred from compression to tension after rotation reverse, but this postulation was not been proven due to inadequate sensitive of downhole sensors. By using an integrated dynamic-behavior sensor with high-frequency sample rate (250 Hz), HFTO ranging from 40 Hz to 90 Hz and beyond has been observed by Pastusek et al. [65], and it seems to be common when drilling hard rocks with PDC bits. Figure 15 shows a 5-second burst data that captured the transition from low state to severe state of HFTO, and this sudden appearance of vibration mode suggests that it is driven by formation and/or operating environment changes but not the result of gradual dulling of bits. A prejob model for a BHA is created by Patil and Ochoa [61] and presumed that the HFTO will occur drilling preidentified formations, and those formations are relatively hard (typically the bulk density is >2.5 g/cc). It has been observed from the downhole memory data recorded by the tools while drilling that severity of the tangential vibration increases when the bit drills through transition zone from the softer porous rock to harder denser one and vice versa.

Based on high-frequency downhole sensors (800 Hz) positioned 1.5 ft (near bit) and 107 ft (drillstring) above the bit, Lines et al. [66] further confirmed the presence of low-frequency (<0.5 Hz) and high-frequency (~70 Hz) RPM periodic oscillation in a BHA including a point-the-bit RSS, respectively, attribute to fundamental torsional nature frequency of drillstring and torsional resonance within BHA. The high torsional resonance with extremely damaging high frequency and magnitude (10000 rad/s^2) is a result of drilling conditions in carbonate formations and has a huge ability to fatigue downhole tools. The occurrence of HFTO is closely related to the downhole tools in BHA. Wilson [63] confirmed that measured HFTOs in motor-assisted rotary-steerable assemblies are associated with torsional resonant frequencies of the BHA's drive shaft, between the motor's power section and the bit. HFTO coinciding with system natural frequencies is also certificated by Oueslati et al. [24], and the dominant mode shape is observed at 174 Hz.

After extensive analysis performed on the downhole high-frequency data, a strong correlation between the occurrence of HFTO and the surface parameters (RPM and SWOB) as well as formations was verified by Zhang et al. [44]. HFTO is normally localized at the BHA, the torsional energy is trapped in a section of BHA, and the frequency of HFTO shifts depending on different downhole conditions. HFTO can be excited and sustained regardless of whether the BHA has a mud motor or not. Low-frequency stick/slip and high-frequency torsional vibration can be excited at the same time and coupled together. HFTO can gradually become increasingly severe which is possibly due to bit wear or motor wear, and severe HFTO with the amplitude of tangential acceleration reach to 200 g peak-to-peak was observed. The results of transient dynamic modeling indicate that HFTO is localized below the motor, and it will not capture the HFTO if a sensor is placed further above the motor. Also drillpipe stopbands were recommended due to the amplitude of HFTO wave decays significantly in it and the energy contained in that natural mode will be trapped. This is very useful in terms of sensor placement and BHA design to reduce the chance of HFTO to avoid premature tool failures.

Shen et al. [62] summarized two mechanisms that cause HFTO to be contained in parts of the BHA or lower drillstring. The first mechanism is associated with rotary drilling without a mud motor, as shown in Figure 16 (upper). The drillstring is assembled from drillpipes with different cross-section areas at the body and tool joint, and this repetitive structure acts as a band filter when torque wave is excited or reflected from the bit and travels up the drillstring. Torque wave with frequencies located in the stop band will be reflected and can cause the torsional vibration energy to be contained in the BHA to develop into HFTO. For this type of HFTO, its frequency is always within the stop band of the drillstring and coincident with one of the BHA's natural frequencies. The second mechanism is associated with

Figure 14: Cracks (45° collar propagating from the collar axis), loose electronic components, and vibration dust induced by excessive HFTO [61, 62].

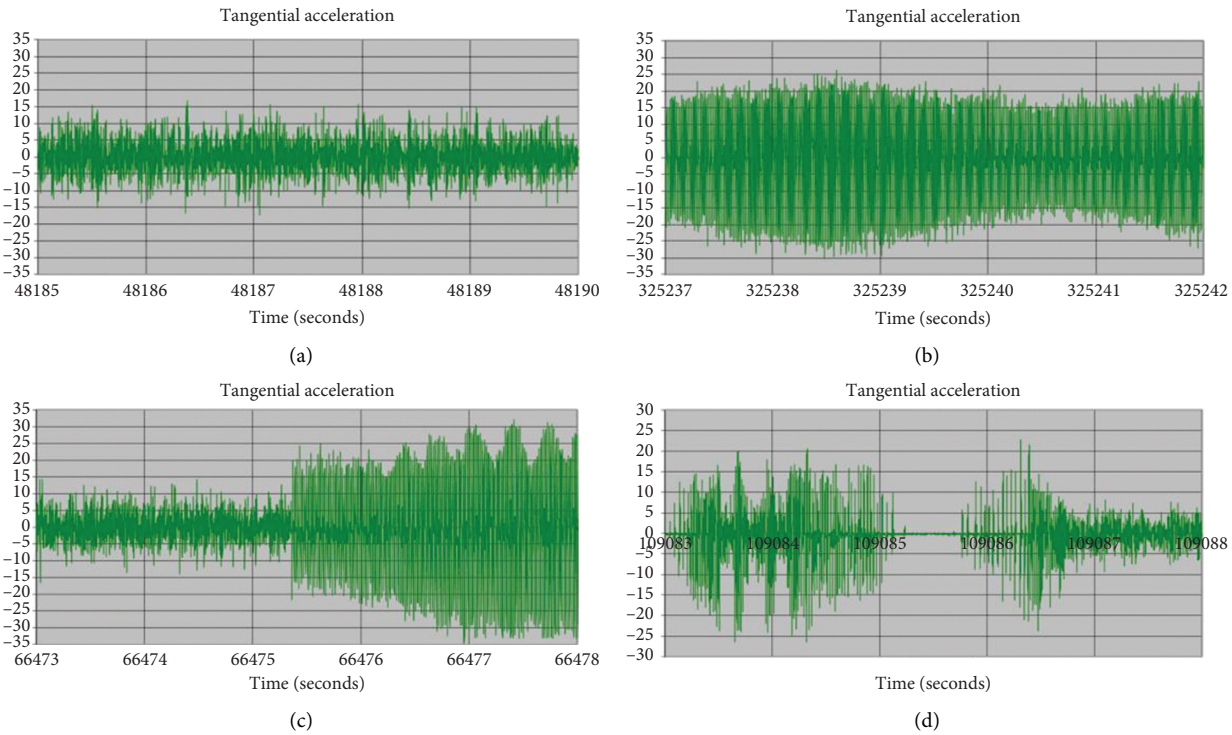

Figure 15: 5-second burst data of different tangential acceleration refer to different states of HFTO [65]. (a) No HFTO; (b) severe HFTO; (c) transition from low HFTO to severe HFTO; (d) two-second period of no bit rotation.

drillstrings with motorized rotary steerable systems as shown in Figure 16 (lower). There is a section of BHA below the mud motor including rotary steerable tools and other components. The mud motor creates a large change of torsional stiffness in the BHA. When the torque wave travels from the bit to the mud motor, the majority of its amplitude will be reflected, and the torsional vibration is contained in the BHA below the motor. This type of HFTO will have frequencies coincident with the natural frequencies of the BHA section below the mud motor.

3.2.2. Models of HFTO. The majority of investigations of HFTO focuses on separated BHA as opposed to the entire system. For this purpose, Tikhonov and Bukashkina [67] built a model that considers the influence of "drillstring-

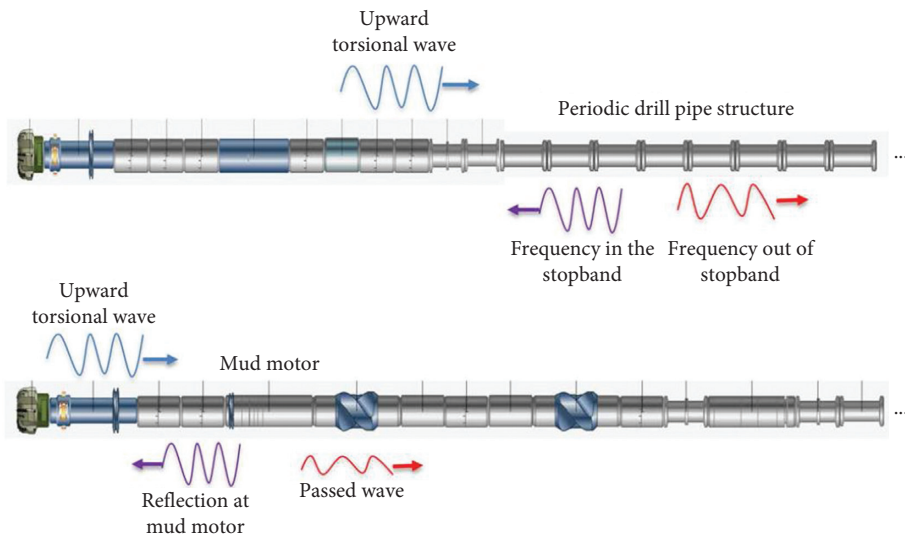

Figure 16: Torsional wave transmission and reflection in RSS BHA without or with mud motor [62].

BHA-positive displacement motor (PDM)-cutting process" in a 3-D well, in which the axial stiffness of drillstring and BHA are taken into account with the axial motion equations coupled with torsional equations, as well as the PDC bit and rock interaction is considered to define WOB and TOB during oscillations. The dynamic equations of the axial force and torque are expressed as equations (1) and (2). The equations of the model can be solved by time integration and harmonic analysis of processes by a computer code called STICK-SLIP2, and then different drilling techniques including rotary drilling, sliding, and combination drilling are analyzed. The results showed that the frequency of HFTO depends on a large extent on PDM dynamics, and the resonance frequency of torsional oscillations while sliding and combination drilling (about 199 Hz) is higher than that for rotary drilling (at 40 Hz). These results will enable drillers to select and adjust drilling parameters to reduce torsional oscillations:

$$m\frac{\partial^2 U}{\partial t^2} - EA\frac{\partial^2 U}{\partial s^2} = q, \tag{1}$$

$$\rho I_p\frac{\partial^2 \Phi}{\partial t^2} - GI_p\frac{\partial^2 U}{\partial s^2} = p, \tag{2}$$

wherein $U = U(s,t)$ is the axial displacement; $\Phi = \Phi(s,t)$ is the rotation angle; ρ is the BHA/drill pipe material density; m is the mass per unit length; E is Young's modulus; G is the shear modulus; A is the cross-sectional area; I_p is the polar moment of inertia; q is the external force per unit length; p is the external torque per unit length; s is the arc position counted off the bottom-hole along the drillstring axis; and t is the time.

A BHA model that could analyze mechanical loading and directional performance of various and dynamic response was developed by Wilson [1]. The model was based on nonlinear finite beam element, and consideration had been given to account for varying mechanical properties, the fully-coupled flexibility of the drillstring, geometric nonlinearity, automatic determination of frictional wellbore contact points with arbitrary radial clearance, three-dimensional wellbore profiles, added fluid mass and damping effects from the hydrodynamic forces generated between the moving drillstring and surrounding fluid, complex tool geometry, shear beam deformations, lateral rotary inertias, and gyroscopic effects. Via equation (3), the linearized vibration amplitude along the BHA could be calculated based on an assumed fluid-damping model and a specific harmonic excitation (bit movement, rotor whirl, etc.). The calculate accuracy of this model was verified by high-frequency field downhole data, the average error of calculated lateral natural frequencies (<5 Hz) was less than 3%, and an even smaller error of calculated HFTO natural frequency was less than 1%:

$$\begin{bmatrix} \underline{\underline{K}} - \omega^2\left[\underline{\underline{M}} + \underline{\underline{M}}_F(\omega)\right] & \omega\underline{\underline{C}}_F(\omega) \\ -\omega\underline{\underline{C}}_F(\omega) & \underline{\underline{K}} - \omega^2\left[\underline{\underline{M}} + \underline{\underline{M}}_F(\omega)\right] \end{bmatrix} \begin{Bmatrix} \underline{\widehat{\psi}}_c \\ \underline{\widehat{\psi}}_s \end{Bmatrix} = \begin{Bmatrix} \underline{F}_{Ec} \\ \underline{F}_{Es} \end{Bmatrix}, \tag{3}$$

where $\underline{\underline{K}}$ is the linearized stiffness of the BHA evaluated at its quasistatic position, $\underline{\underline{M}}_F(\omega)$ is the frequency-dependent fluid-mass surrounding the drillstring, $\underline{\underline{C}}_F(\omega)$ is the frequency-dependent fluid damping, ω is the circular excitation frequency, $\underline{\widehat{\psi}}$ is the calculated dynamic displacement vector, $\underline{F}_E$ is the excitation force vector, and the subscripts c and s are cosinusoidal and sinusoidal terms, respectively.

To address the challenges brought by HFTO, a method for automated BHA optimization based on mechanical drillstring models was proposed, as well as a criterion for the prediction of the excited torsional mode and the corresponding loads (acceleration and torsional torque) was derived by Hohl et al. [68, 69]. The criterion is based on the comparison of the resulting excitation from cutting forces at the bit and the damping of a torsional mode, and it is unique for every torsional mode and can be used to rank the susceptibility of torsional modes for HFTO and stick/slip. The

stability state can be judged by a critical value obtained from equation (4), and the torque characteristic dTorque/dRPM has to be greater than the critical value $S_{c,k}$ for every mode shape k to achieve stable drilling. The modeling results showed that an increase of bit inertia and outer diameter of the collars between the bit and the motor results in increasing stability, and slight changes in the BHA design significantly increase stable drilling with respect to HFTO. It is further revealed that stick/slip can be reduced by selecting stiffer drillpipe with bigger outer diameter, but the length of drillpipe has a negligible influence on the stability of stick/slip and HFTO. Based on this model, a software application called Torsional Oscillation Advisor (TOA) had been developed and provided valuable input for drilling optimization. The analysis results show that the material and mass of bit distribution is shown to have a considerable influence on the excitation of HFTO. It must be noted that this behavior was expected because the amplitudes of HFTO are theoretically linearly scaled by the rotary speed at the bit [70]:

$$S_{c,k} = -\frac{2D_k\omega_{0,k}}{\varphi_k^2} < \frac{\text{dTorque}}{\text{dRPM}}, \tag{4}$$

wherein D_k is the modal damping of the considered torsional mode, $\omega_{0,k}$ is the angular eigenfrequency, and φ_k is the deflection of the mass normalized eigenvector at the bit.

Though the combined measurement of tangential acceleration and dynamic torsional torque gives a sound estimation of the severity of HFTO at measurement position, representative and comparable values that are the maximum value of tangential acceleration and dynamic torsional torque that are present in the BHA are still not unveiled. The derivation of a representative value for the severity of HFTO is independent of the sensor position, but the measurement signal is very sensitive with respect to the distance from the bit of the sensor placement if only one mode shape is dominantly excited. To overcome this limitation, an approach to calculate the maximum of the tangential acceleration and the dynamic torsional torque amplitude for one mode is proposed by Hohl et al. [70], and the measured signals of tangential accelerations and dynamic torsional torque are combined to a representative value, which is independent of the measurement position and characterizes the severity of HFTO. These values can be calculated by algorithm implemented in MWD tool and can be sent to the surface in real time. In comparison with the traditionally derived root mean square value of the tangential acceleration measurement at the sensor position, the approach delivers values that are factors higher, which can indicate high levels of HFTO while the traditionally values cannot. These results in the application enables the driller or an automated advisory system to initiate the optimal HFTO mitigation strategy that leads to reduced levels of vibration with the known benefits for the cost of a well.

A system model for HFTO mitigation is built considering the entire drilling system including the bit-rock interaction, downhole drive(s), BHA design, and surface drilling parameters by Shen et al. [62]. This 3D transient drilling dynamic model was developed for mud motors and rotary steerable system (RSS) tools, and it had been extended to study the severity of HFTO and cyclical loading to drilling tools. After conducting a full drilling simulation, the drilling system behavior under HFTO can be fully described. It was found that cyclical torque loading of differing magnitudes and frequencies were observed for different BHA components depending on HFTO vibration mode, HFTO severity, and BHA design. The simulation results show that high-frequency loading variations are experienced by the joints on both ends of the transmission shaft and high-frequency torque variation is also observed on the rotor, with higher amplitude close to the lower end. This can cause accelerated wear and tear on those joints and the rubber material to undergo high-frequency cyclical loading, which accelerates wear and tear on the rubber material together with the RPM difference between the rotor and stator.

3.2.3. Severity Evaluations of HFTO. Based on utilizing field and laboratory testing with high-frequency sensors, Oueslati et al. [41] summarized a stability map of HFTO (see Figure 16) under different WOB and RPM. Figure 17(a) shows that low- and high-amplitude vibrations distinctly fall into zones, which indicate that HFTO occurs at higher WOB and low-to-moderate RPM. Figure 17(b) shows that the HFTO corresponds to the higher frequencies, occupying majority of the smooth drilling zone and part of expected stick/slip, which confirms that HFTO typically does not occur in the low WOB-high RPM zone of backward whirl. HFTO often corresponds to efficient drilling parameters in a given hard formation and does not seem to adversely affect the drilling efficiency, and the stick-slip does not affect the occurrence of HFTO. Thus, it is unsuitable to mitigate HFTO by adjusting the operating parameters because such adjustment may lead to inefficient drilling and trigger other more damaging dynamic dysfunctions.

Through data collected from the DDS in RSS and motorized RSS (MRSS) BHA runs, the relationship between the drilling parameters (WOB and RPM) and the tangential vibration was plotted by Patil and Ochoa [61], as shown in Figure 18. High tangential accelerations are recorded as the WOB increases and also has liner relationship with RPM, and it could be concluded that these are primordial parameters for this drilling dysfunction triggered by HFTO. Figure 18(a) shows that higher WOB and RPM are applied to improving drilling performance while drilling with RSS BHA, but resulting in higher amplitudes for the tangential acceleration. Figure 18(b) shows the effect of WOB and RPM on tangential vibrations for an MRSS BHA, and due to decoupling effect of tangential vibration in the presence of the downhole motor, less surface parameters are applied to improving drilling performance when compared with the RSS BHA given the same formation. It is obvious that understanding the relationship of HFTO occurrence within the given formation and drilling parameters provides crucial information while planning for a job in harder formation.

The model proposed by Shen et al. [62] can be used for sensitivity studies to evaluate the HFTO risk for different

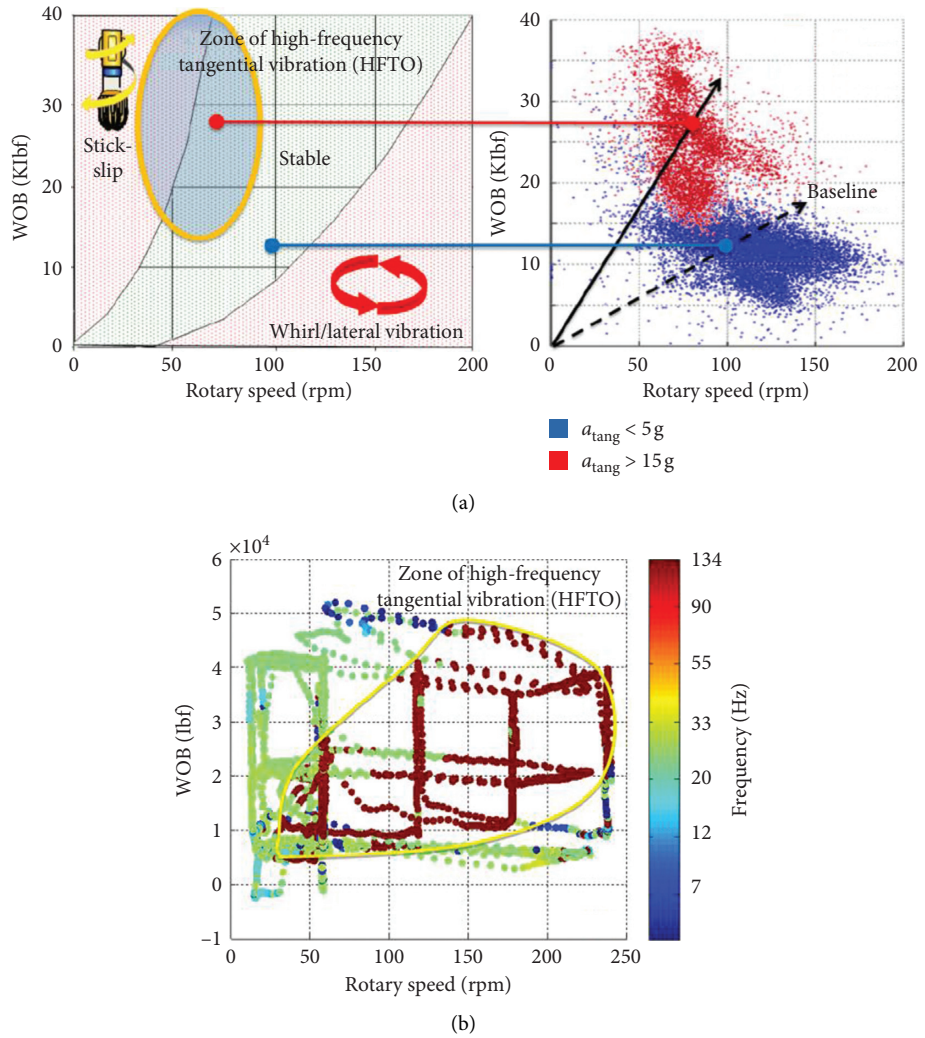

Figure 17: Stability map of HFTO in the field (a) and in the lab (b) [41].

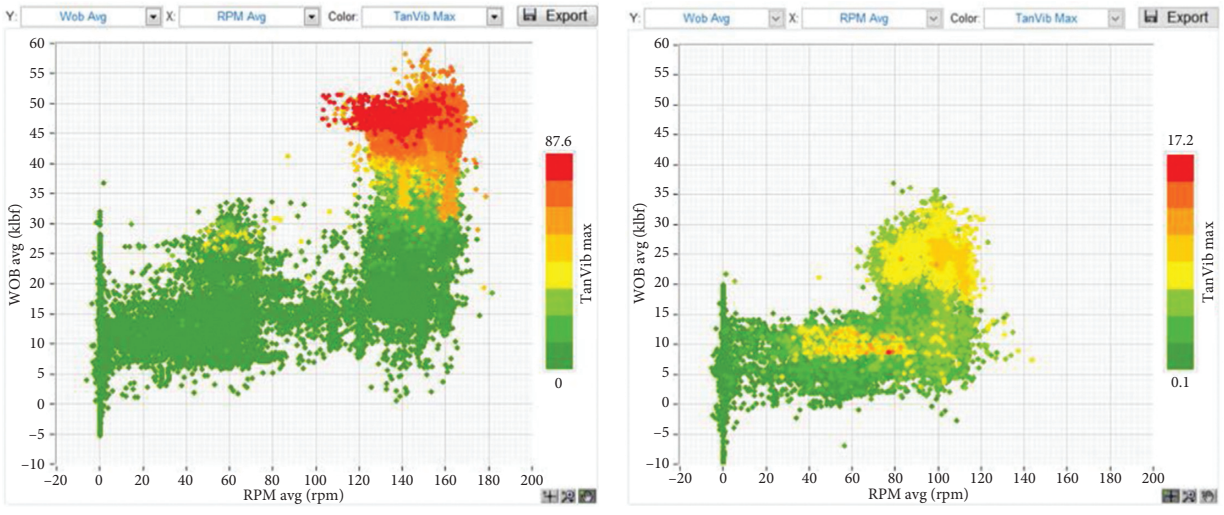

Figure 18: Cross-plots showing relationship between drilling parameters (WOB and RPM) and tangential vibration from downhole memory data for (a) RSS BHA and (b) MRSS BHA [61].

drilling system designs, and the results are shown in Figure 19. It shows that a mud motor with a stiffer power section can reduce HFTO severity because a portion of the HFTO energy can leak into drillstring section above the motor and be damped out. High WOB is more likely to excite HFTO. HFTO can also be affected by bit designs. In parallel to this work, Shen et al. have been evaluating high-frequency downhole measurements through tens of thousands of runs for HFTO, which provided insights of the real reach of the disfunction. One example of the study is shown in Figure 20. The horizontal axis is the drilling performance indicator with unit m^2/s as defined in equation (5), the higher the better. The vertical axis is bit dull indicator as defined in equation (6), the lower the better. The color indicates the ratio of high-frequency datasets with HFTO recorded by downhole sensors. The large datasets showed that HFTO is correlated with poor drilling performance and there is also a correlation of severe bit dull with HFTO. These results can help us manage the disfunction effectively and towards achieving uncompromised drilling performance:

$$\text{Drilling challenge} = \text{drilling distance} \times \text{on} - \text{bottom ROP}, \tag{5}$$

$$\text{Bit IADC inner and outer} = \frac{\text{Bit IADC inner} + \text{Bit IADC outer}}{16}. \tag{6}$$

3.3. New Types of High-Frequency Axial Vibrations. A new type of high-frequency axial vibrations called high-frequency axial oscillations (HFAOs) was verified by Sugiure and Jones [71] using high-frequency dynamic sensors embedded into different positions of a motor-assist RSS BHA during drilling in shale, and the frequency of HFAO is 33 Hz and 203 Hz, as shown in Figure 21. The 203 Hz HFAO along with the 114 Hz HFTO and its second harmonic (228 Hz) can be observed in the axial-acceleration spectrogram, and the reason is considered that the HFTO appears slightly on the axial accelerometers due to the mechanical interaction between axial and torsional/tangential motions. On account of the axial oscillation tends to be more resonated at around 200–230 Hz in this particular BHA and drilling condition (especially the bit-formation interaction), the second harmonic of the HFTO (228 Hz) appears stronger than the 114 Hz HFTO signal. Less research of HFAO can be found out, but it can be seen that the HFAO and HFTO have interactions.

3.4. Coupling of Vibrations and Motions. It is well known that different modes of downhole shocks and vibrations can couple to one another. For example, severe bit bouncing may tend to bend the drillstring and generate lateral vibration. The coupling of longitudinal, transverse, and torsional drillstring vibrations at low frequency less than 10–20 Hz is widely discussed by researchers, and LFTO and stick-slip modes could couple to axial vibration mode. The limitation of low-frequency oscillations was broken through by high-frequency measurements, and new insights were provided to explore the coupling between different kinds of low-frequency oscillations, high-frequency oscillations and low-frequency oscillations, and different kinds of high-frequency oscillations.

3.4.1. New Insight of the Coupling of Whirl and Stick-Slip. A kinematic model of whirl was built by Baumgartner and Oort [25] which was verified based on high-frequency data, and then the observations of coupling of whirl and stick/slip in field data were researched by simulations. The field data and simulation results of radial accelerations during a long stick/slip cycle (period of 8.5 seconds) are shown in Figure 22. Just as the RPM picks up, typical whirl patterns appear, and the fluctuations show a lower amplitude when a certain speed is reached and increase again at the end of the slip cycle with low RPM. The right side of figure shows a simulation using the kinematic model and varying RPM inputs. In the upper plot, the amplitude reaches from zero to its maximum value, while in the bottom plot, the amplitude fluctuates between two high-acceleration levels, which is coincided with the field data suggest that one or more parameters change within the stick/slip cycle and thus cause the change in whirl amplitude. The high velocities during stick/slip have a stronger influence on the radial than on the tangential component. High-amplitude tangential fluctuations therefore are more likely to be attributed to lateral vibrations rather than higher-frequency torsional vibration phenomena.

3.4.2. Coupling of High-Frequency Oscillations and Low-Frequency Oscillations. (*1) The Coupling of HFTO and Stick/Slip*. According to Lines [72], the low-frequency torsional oscillation (LFTO) and full stick/slip typically occur at less than 2 Hz, HFTO occurs between 50 and 250 Hz, and the three modes may also occur simultaneously. Actually, the simultaneous LFTO and HFTO could interact with each other. Patil and Ochoa [61] put out a chapter of high-speed data from the tool's memory (Figure 23), and the left graph shows continuous HFTO while the right picture shows stick-slip superimposed on HFTO. These high-torsional frequencies attenuate the resultant torque and RPM values causing angular displacement that results in significant amount of shear strain within the BHA.

Strong coupling between low- and high-frequency torsional oscillation was observed by Zhang et al. [44]. A data slot that vibration becomes more severe is shown in Figure 24 (Figure 24(a)). It can be seen that, as the bit/BHA slips, both amplitudes of the RPM and tangential acceleration increase dramatically. During the slip phase, the bit is

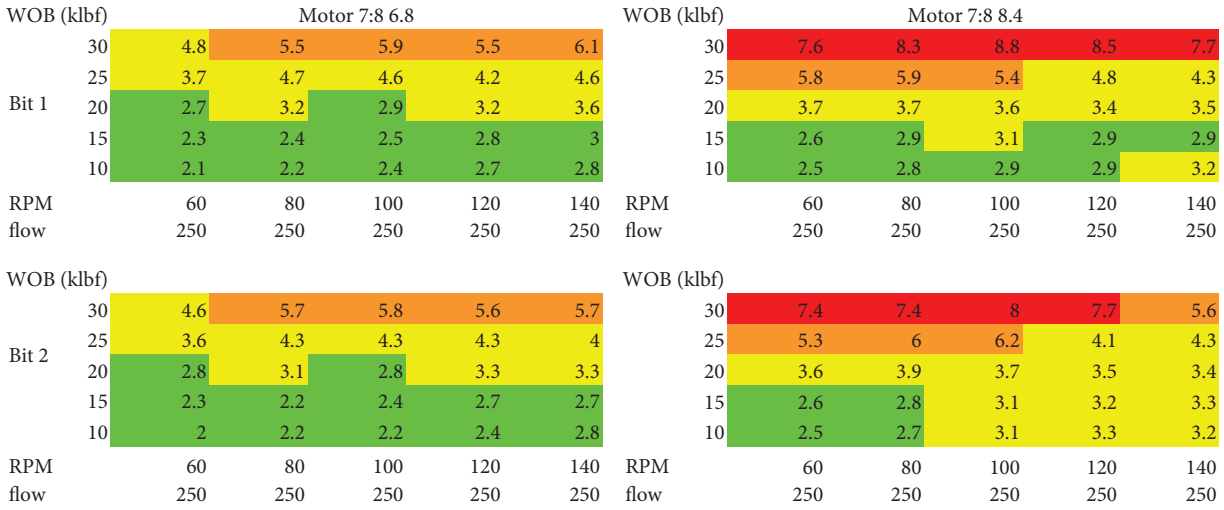

Figure 19: Results from HFTO sensitivity study by Shen et al. [62].

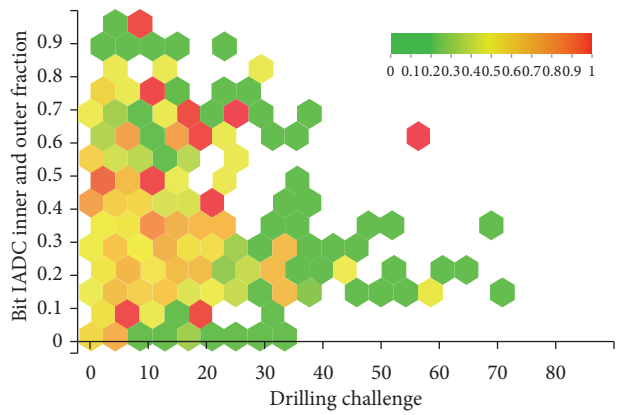

Figure 20: Bit dull, drilling performance, and HFTO [62].

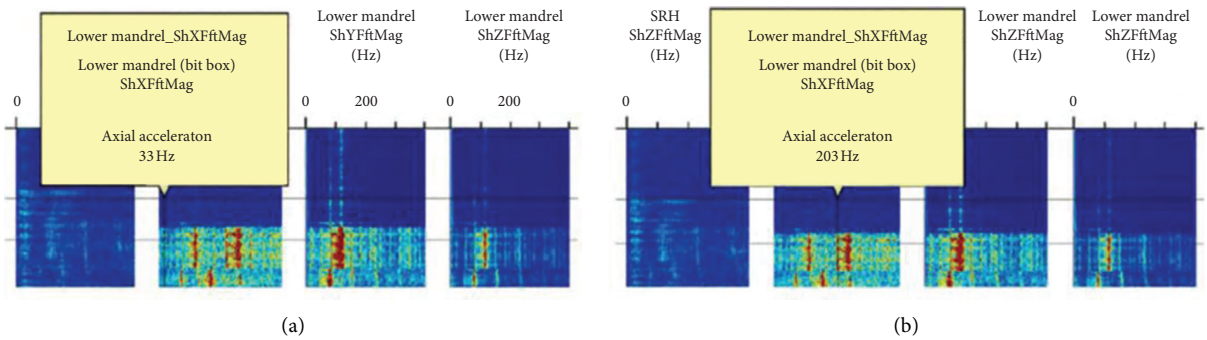

Figure 21: HFAO spectrogram with frequency of 33 Hz (a) and 203 Hz (b) [71].

cutting the formation, thus the forces generated by the bit rock interaction are the likely excitation source of HFTO. When bit comes to a stop, such excitation source is temporarily removed, causing the reduction of tangential acceleration amplitude. The maximum tangential acceleration reaches as high as 100 g during the slip phase, while the downhole RPM spikes up to 600 rpm. Furthermore, Figure 24 (Figure 24(b)) presents a zoomed view of the data to two stick-slip cycles. The HFTO has a dominant frequency at 194 Hz was coupled with a 7-second stick/slip. The measured 194 Hz is one of the natural frequencies of the substructure below the motor, while the stick-slip frequency is the first fundamental frequency of the entire drill string. Surprisingly, quite high negative downhole RPM was

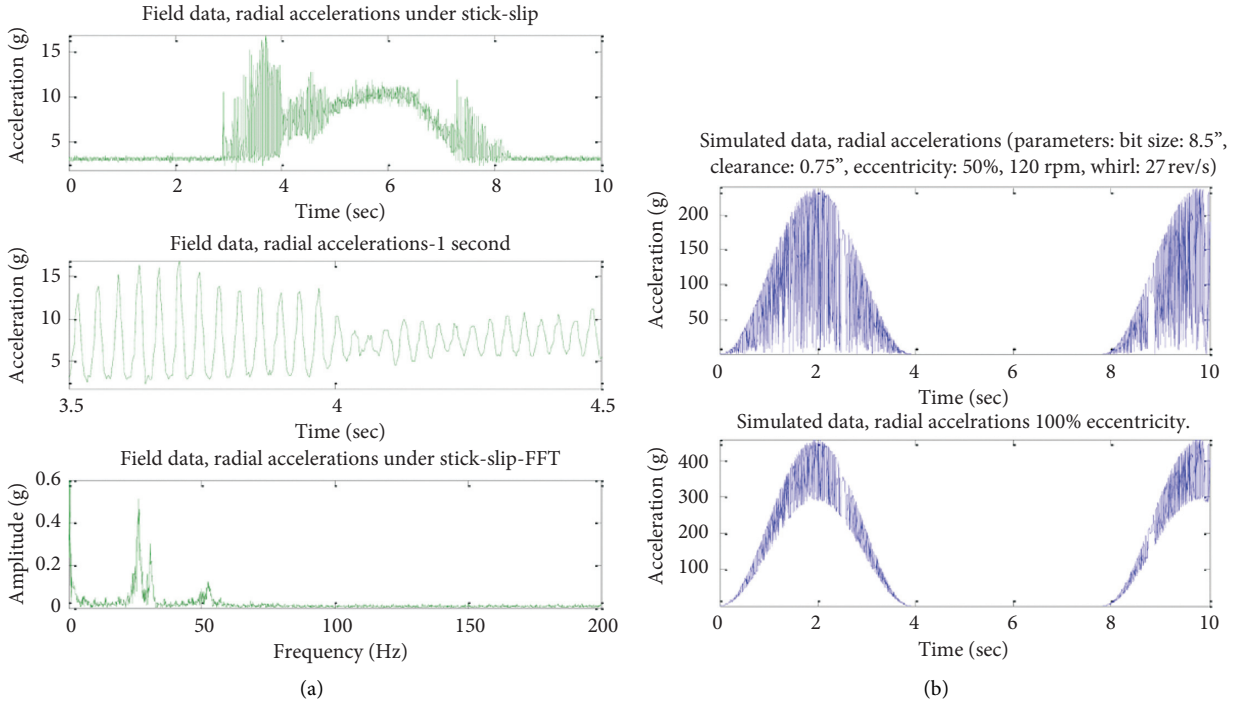

FIGURE 22: Radial accelerations of field data (a) and simulated data (b). The simulation is done with 50% eccentricity and 100% eccentricity [25].

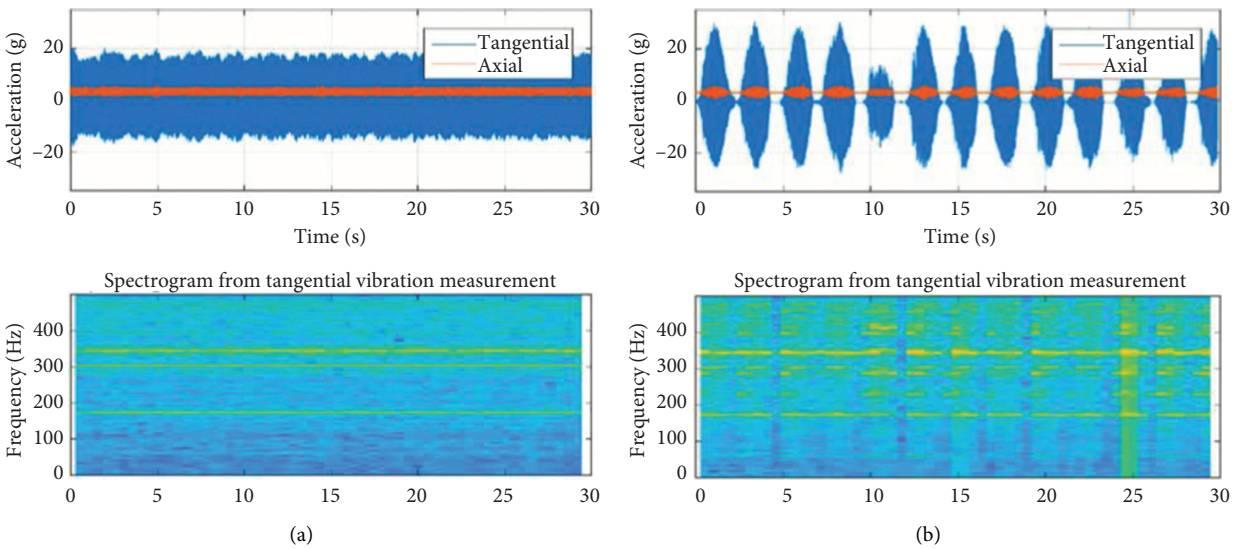

FIGURE 23: HFTO scenarios: (a) high-frequency torsional resonance and (b) HFTO with stick-slip [61].

observed during severe HFTO, as the exact same trend as tangential acceleration. The amplitude of the torque variation gradually increases throughout the run which may be a sign of the aggravation of HFTO. Figure 25 zooms in a section of 3-second data, and it shows that large negative spikes are generated during HFTO and a 15 kft-lbf peak-to-peak torque amplitude was observed. Due to the high frequency, this can consume the fatigue life of downhole tools at a much faster rate. FFT is performed, and a dominant frequency of HFTO at 149 Hz is found, which was also coupled with axial motion and axial loading.

Field continuous downhole data showed scenarios including pure HFTO and stick-slip with superimposed HFTO were discussed by Hohl et al. [73], the results show that the stick/slip and HFTO interact with each other, and the large frequency gap between them allows for different effects and excessively increasing loads. During a period of stick/slip, the low-frequency bit rotary speed tends to change and very

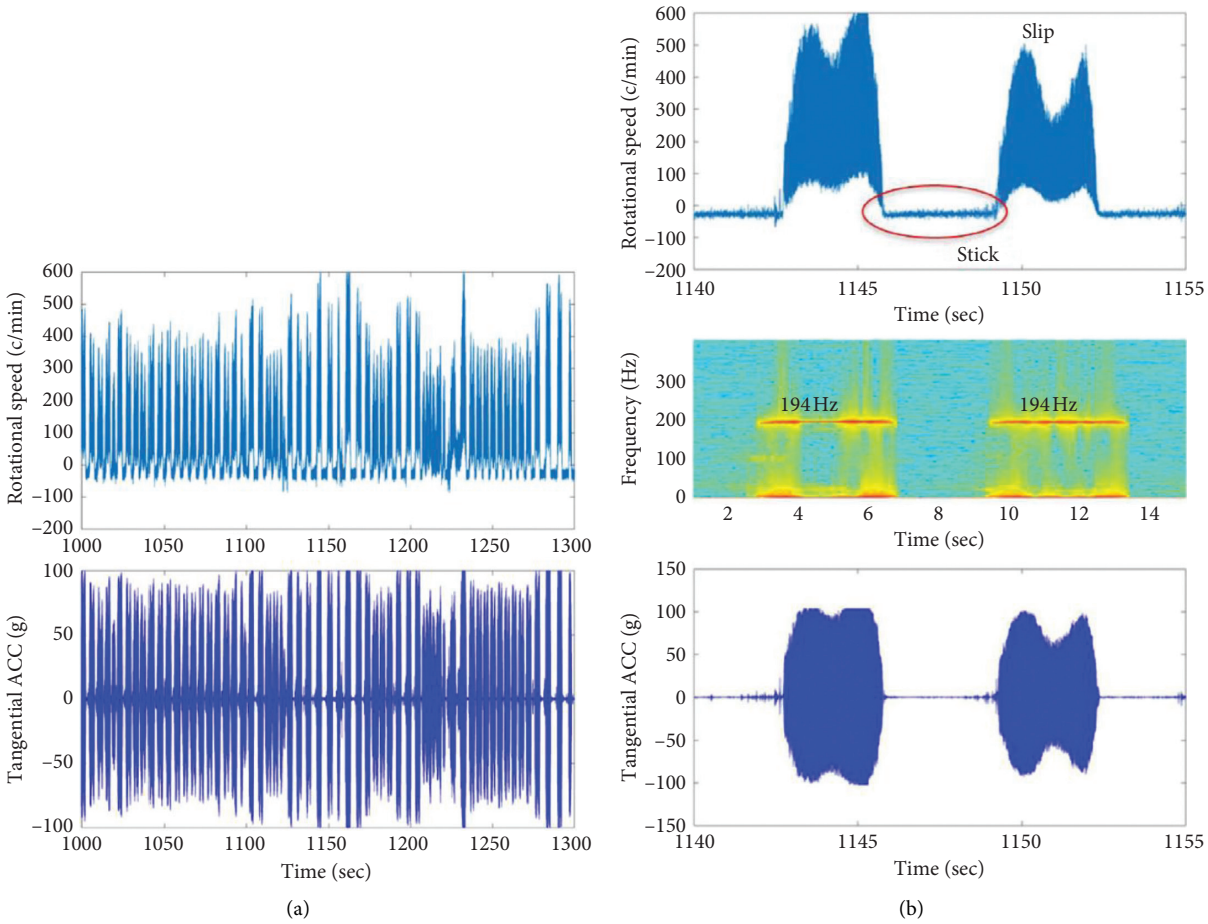

Figure 24: Coupled HF and LF torsional oscillation (a); zoomed view of coupled HF and LF torsional oscillation (b) [44].

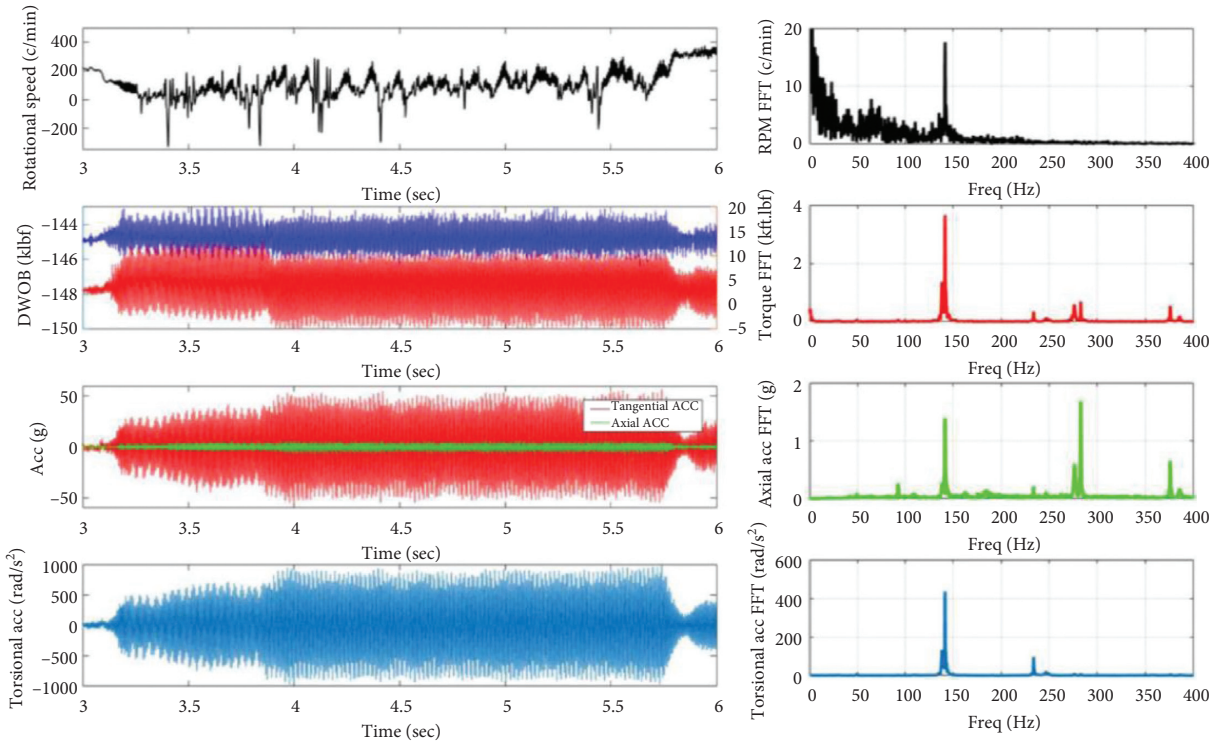

Figure 25: Zoomed view of the high-frequency data and FFT of the high-frequency data [44].

high values of the rotary speed can be achieved in the slip phase if HFTO is more unstable and associated loads increase very fast lead to excessive loads. However, stick/slip can also be beneficial from a purely HFTO driven perspective. The stick phase reduces the HFTO-related torsional amplitudes to zero. The speed of increase of HFTO can be very slow, and therefore, the worst-case amplitude might not be reached before the increasing amplitudes are again interrupted by the declining bit rotary speed and the stick phase. The stability of HFTO and stick/slip is mapped in Figure 26, and different mitigation strategies for specific scenarios could be presented to reduce the field loads associated to HFTO. Though the strategies sometimes may be compromised to actual drilling situations, derivation of general rules for HFTO mitigation strategies uses the results and observations from the analysis unveils optimization opportunities for drilling efficiency and ROP.

Additionally, the HFTO is not only coupled with stick-slip but also interacted by backward rotation. By drilling dynamic data sampled at 1600 Hz, HFTOs with frequencies above 400 Hz and backward rotation were observed by Sugiura and Jones [31]. These HFTOs mostly appear with low amplitudes (10 to 50 g) from conventional steerable motor runs and high amplitudes (100 to 200 g) from motor-assisted RSS runs. It is noticed that extreme multiaxis high-shock events (caused bit temperature rises) occurred at the beginning of the slip phase (0.18 Hz LFTO) and a very strong 560 Hz HFTO always presents while the bit rotation speed slowly varied. The amplitude of this 560 Hz HFTO is lowest at 80 rpm and highest at 250 rpm, which is highly correlated with the bit rotation speed. In this case, no HFTO dominant frequency shift was observed while the bit rotation speed widely varied, indicating that the dominant frequency of HFTO is independent of the bit rotation speed, but the phenomenon of switching between LFTO and HFTO was also repeatedly observed. The bit dysfunction completely switches to HFTO when LFTO stopped, which was thought to come from the formation changes and with no clear correlation with the surface parameters. Interestingly the dominant frequency of HFTO can switch while LFTO happens. The phenomenon that the dominant frequency of HFTO switched from 76 Hz (second-order mode) to 114 Hz (fourth-order mode) with no visible change of surface parameters (RPM, WOB, flow rate, etc.), ROP, and total gamma-ray-count (formation information) is observed, while LFTO is quite visible in the bit-box RPM. The HFTO frequency shift which indicates the HFTO severity is highly correlated to the nominal bit rotation speed.

3.4.3. Coupling of High-Frequency Oscillations. For enhancing the understanding of HFTO of BHAs, an integrated analysis considering rock, cutter, bit, and BHA interaction was presented by Jain et al. [74] from laboratory/field testing and computer modeling. Jain et al. proposed that HFTO is a result of bit-induced high-frequency torsional resonance in the BHA and occurred at much higher frequency (130 Hz and 245 Hz) than reported before or the fundamental mode of the BHA, the amplitude of HFTO typically increases with RPM and WOB because of additional power input, and they are strongly coupled with axial vibrations that occur at the same frequency (as shown in Figure 27). Though the HFTO is induced by cutting action is confirmed and PDC cutters can come to a momentary stop during HFTO, the design of bit does not significantly affect the occurrence of HFTO and the likelihood of PDC cutter damage from backward motion during HFTO is low. The modes most susceptible to exhibiting HFTO can be identified, and the dominant mode is predicted, which provides a basis for tools and BHA design that avoid or withstand the HFTO.

The coupling of HFTO and HFAO was also observed by Sugiure and Jones in different shale formations with a motor-assisted RSS BHA [71], and the third-order-mode HFAO and the harmonics of the HFTO coupled to the longitudinal axis were discovered. As shown in Figure 28, the 114 Hz HFTO and its harmonics (e.g., 228 Hz and 342 Hz) are directly coupled to the axial channel, and the magnitude of the axial vibration coupled from the harmonics of the 114 Hz HFTO is higher than that of the 203 Hz third-order mode HFAO. Due to the bit area suffers the highest accelerations in any mode numbers and both torsional and axial modes, it is more typical to observe high degrees of mode coupling with recorders installed below the motor than the sensors deployed in the motor top subs and drillstring subs. In drillstring subs, the HFAO also can be also observed with a dominant frequency; however, the axial vibration mode is suppressed and switched over to torsional mode when the torsional mode is more excited. Additionally, HFTO-damping effect was confirmed while drilling with the slow-rotating housing of the RSS rotating freely, a torsional mass damper, torsional friction damper, torsional viscous damper, and a combination of these are all viable options for downhole HFTO mitigation, which allow us to optimize the surface parameters for maximum ROP and reducing BHA failure.

4. Applications Based on High-Frequency Measurements

By using high-frequency measurements, the understanding of drillstring dynamics is investigated in greater detail. As a result, drilling engineers are able to gain new evidences into monitoring dynamic dysfunction and making optimization strategies. Based on models and theory analysis using high frequency mentioned above, ways to minimize or utilize drillstring dynamics to improve drilling performance are proposed. Although in some cases the goal is to maximize dynamic response (for example, when introducing oscillation tools to overcome wellbore friction while directional drilling or to free stuck pipe), usually the goal is to minimize dynamic response to limit the effects of potentially damaging phenomena in the low-frequency and high-frequency range, led to resist whirl, mitigate stick-slip, avoid HFTO, and so on. Besides, by identifying high-frequency data collected downhole, the formation can be classified.

4.1. Ways to Minimize Vibrations. Lines [72] proposed that novel torque-limiting downhole tools can be very effective at combating the severity of bit-induced full stick-slip and HFTO, like Weatherford's latest torque-limiting tool, which is a purely mechanical device placed above the BHA and extends/contracts

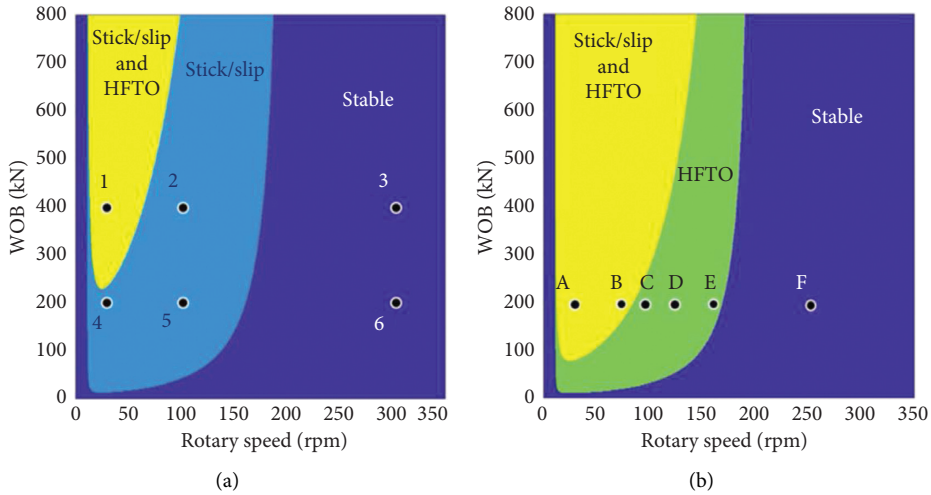

Figure 26: Stability map for stick-slip and HFTO with dominant stick-slip (a) and dominant HFTO (b) (yellow: unstable areas for stick/slip and HFTO, green: unstable area HFTO only, light blue: unstable area stick/slip only, and dark blue: stable area) [73].

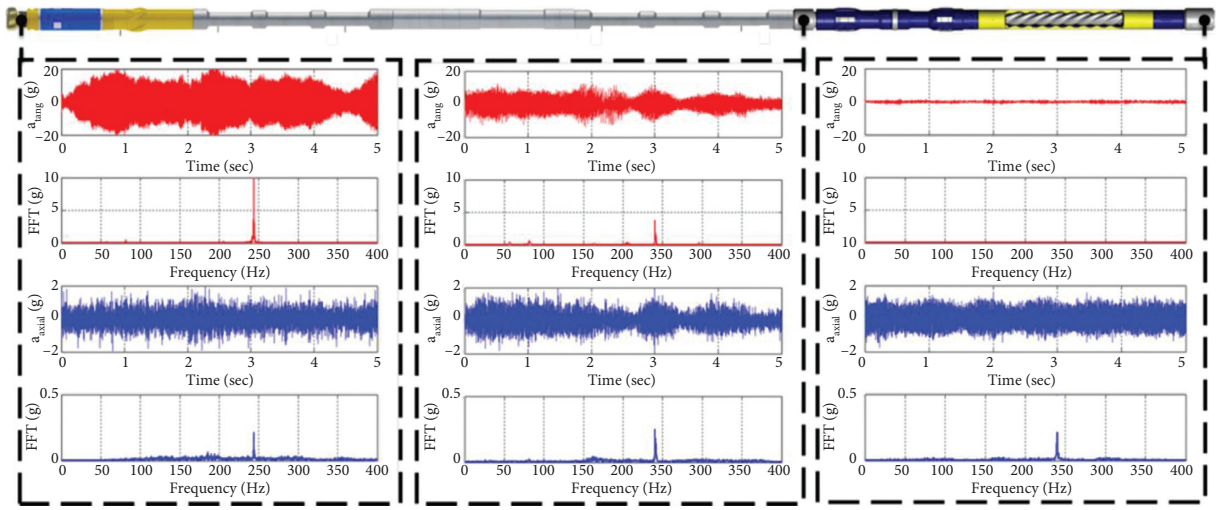

Figure 27: High-frequency data recording of torsional (red) and axial (blue) acceleration at three different positions of the RSS BHA and FFT analysis of the signals [74].

in response to drill-bit torque. The extension and contraction moderate bit engagement with the rock face, contracting as the drill bit begins to torque up and preventing a full stick, then extending during the slip (or high-RPM) phase to allow the bit to remain engaged as the rate of rock removal increases. These tools, such as PDMs, also act as low-pass filters and can be used to isolate sensitive BHA components from HFTO.

PDM employed to perform as an additional torque source near the bit was also reported by Hoffmann et al. [42]. In-bit high-frequency data showed that severe stick-slip occurred in 8 $^{3}/_{4}$ in. and 12 $^{1}/_{4}$ in. vertical sections of horizontal wells when drilling in very hard rock with a conventional rotary assembly (PDC bit). While drilling at 60 rpm with 110 kN WOB at the surface, severe stick-slip near bit makes the RPM peaks rise to nearly 500 rpm. After bringing a PDM into BHA, the RPM fluctuations turned smooth and the observed occurrence of stick-slip vibrations was reduced to only 15% of the time, by which the cutters damage was solved effectively.

Based on the knowledge gained in bit dynamics and cut damage from case study, a new superior bit design with more stable cutting structure specifically for mitigating lateral vibration and reducing backward whirl damage for the challenging offshore application is designed by Oueslati et al. [24]. Depth of cutting control feature placement was also enhanced to address stick/slip issues, and a new generation of cutters with superior technology and more robust diamond table was deployed to improve PDC cutter durability and bit life. The new bit design achieves 30% better ROP and 26% longer runs than old design, as shown in Figure 29.

Although HFTO can be measured and its effect is modeled and predicted, little can be done to mitigate HFTO while still maintaining efficient drilling, a string component with certain mass and stiffness properties could be used to isolate a portion of the BHA from HFTO. Based on restricting potential damaging HFTO vibrations to a part of the BHA that is designed strong enough to survive HFTO, tools for

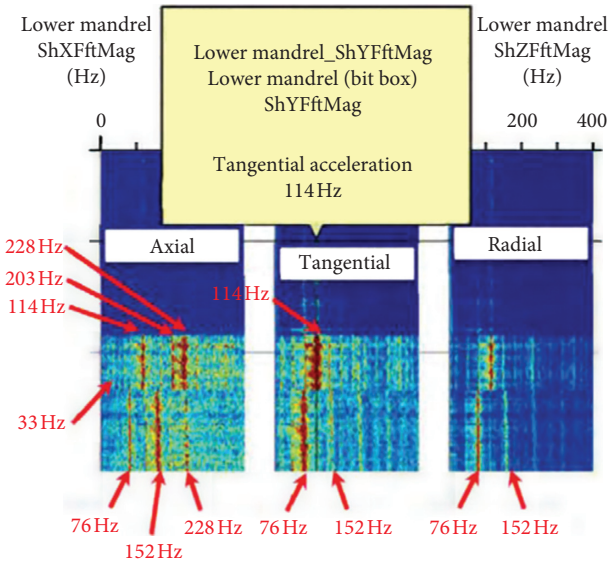

Figure 28: Coupling of HFTO and its harmonics to the axial channel [71].

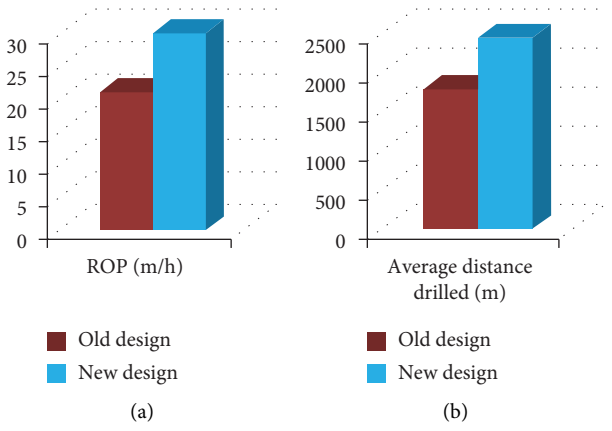

Figure 29: Performance comparison of the old and new bit design established from ROP (a) and distance drilled (b) [24].

isolating HFTO from the lower to the upper part of the BHA have been developed by Heinisch et al. [75] and Carpenter [76]. By using this isolator tool, the BHA is modified so that critical HFTO mode shapes only have significant amplitudes in the section below the isolator tool, preventing the propagation of higher-frequency torsional vibrations upward the BHA and string, as shown in Figure 30. The isolator tool significantly improves the performance and reliability of MWD and LWD tools and reduces damages and consequent failures caused by HFTO, therefore resulting consistently in longer runs, reduced NPT and minimized cost per foot.

4.2. Drilling Formation Predict. Changes in drilling system dynamics driven by the bit's interaction with the formation will be a near instantaneous indicator of changes in formation characteristics and properties [57]. For a sensor located near the bit, the spectrum is dominated by the resonances of the BHA and bit-rock interaction. The BHA remains constant during the duration of a bit run; thus, frequency shifts indicate formation changes and can be used to identify formation tops [59]. Figure 31 [77] shows the original vibration signal (time series sampled at 40 kHz) of orthogonality directions during cutting conglomerate rock

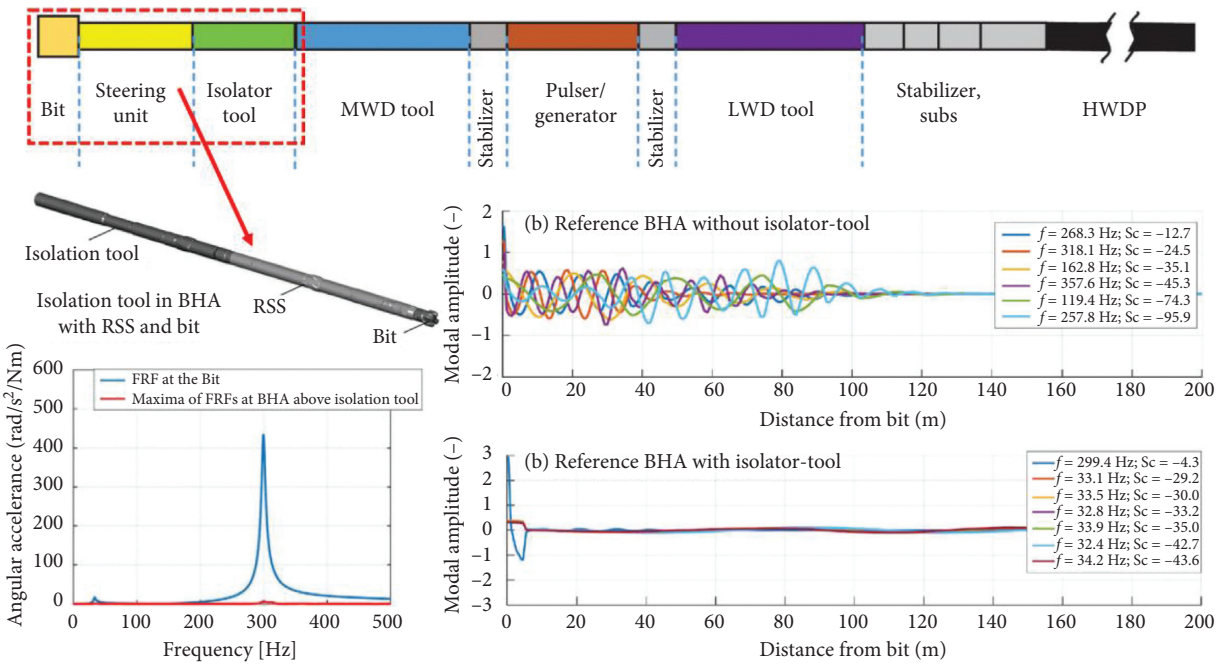

Figure 30: The isolator tool comprised in a typical field BHA and its effect [75, 76].

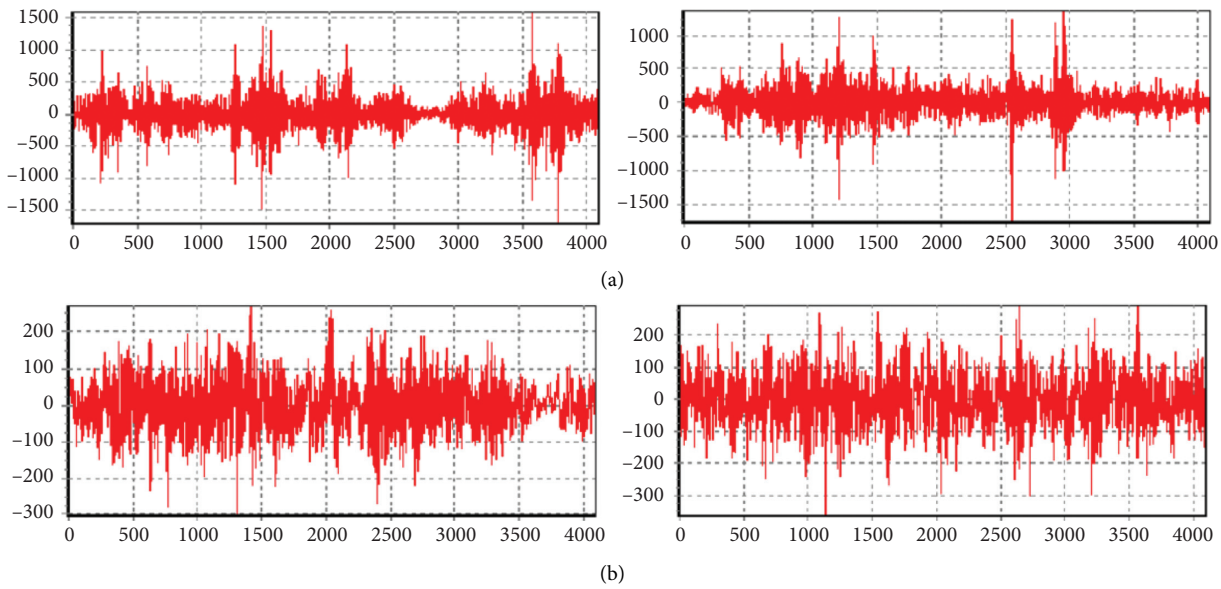

Figure 31: The original vibration signal during cutting conglomerate rock (a) and sand-mudstone (b) [77].

(top) and sand-mudstone (bottom), and it can be see that the vibration energy of conglomerate rock is obviously large than sand-mudstone. There are singularity signals with high values in the signal of conglomerate rock, and these kinds of signals can be used to lithology identification.

5. Conclusion

The wealth of information provided by high-frequency dynamic data, which are not present in low-frequency data, offers the possibility to significantly improve vibration mitigation and control methods. This, in turn, provides opportunities for step-changes in drilling performance improvement. Until recently, high-frequency data are not yet used to its full potential, as the industry is only just beginning. Through modellings, simulations, and field tests, the exact source of the HFTO is still unclear; further work is still needed to reveal the relationship of HFTO to bit characteristics such as bit aggressiveness and angular location of bit blades. Further investigation on detailed mechanical components in the BHA and geophysical/geomechanical parameter changes in lithology will be required. In fact, obtaining accurate

measurement of individual vibration components along the drillstring or at the bit is remaining a challenge, especially in applications requiring that BHA configuration and hydraulic horse power at the bit are minimally disturbed. Advanced sensors, high-performance tools, high-speed transmission, new standardized calibration devices and procedures, powerful software, and optimized data processing technologies are urgently needed. There still seems to exist a large gap between the research perspective and practical perspective, the drillstring dynamics remains unpredictable or even undetectable, and even the causes, influence factors, and control application state of drillstring dynamics leave space for disagreements and disputes.

Conflicts of Interest

The authors declare that there are no conflicts of interest regarding the publication of this paper.

Acknowledgments

This work was supported by a grant from the National Key R&D Project of China (grant nos. 2019YFB1504102 and 2018YFC0604302) and Basic Research Fund of Chinese Academy of Geological Sciences (grant nos. JYYWF20180501 and JKY202008).

References

[1] J. K. Wilson, "Field validation of a new BHA model and practical case studies in unconventional shale plays, with a framework for automated analysis for operations support," in *Proceedings of the SPE/AAPG Eastern Regional Meeting, SPE-191780-18ERM-MS*, Society of Petroleum Engineers, Pittsburgh, PA, USA, October 2018.

[2] J. K. Vandlver, J. W. Nicholson, and R.-J. Shyu, "Case studies of the bending vibration and whirling motion of drill collars," *SPE Drilling Engineering*, vol. 5, no. 4, pp. 282–290, 1990.

[3] H. Reckmann, P. Jogi, F. T. Kpetehoto, S. Chandrasekaran, and J. D. Macpherson, "MWD failure rates due to drilling dynamics," in *Proceedings of the IADC/SPE Drilling Conference and Exhibition, SPE-127413-MS*, Society of Petroleum Engineers, New Orleans, LA, USA, February 2010.

[4] R. D. Zhu, P. Chen, J. L. Zhou, and X. Li, "The development of a downhole tool used in deep water top hole drilling that can measure pressure and temperature while drilling," *Machinery*, vol. 1, no. 1, pp. 93–95, 2012.

[5] Q. Xue, H. Leung, L. Huang et al., "Modeling of torsional oscillation of drillstring dynamics," *Nonlinear Dynamics*, vol. 96, no. 1, pp. 267–283, 2019.

[6] C. Yang, P. Chen, H. Xia, X. Han, and T. Ma, "Progress in research and development of measurement-while-drilling apparatuses," *Natural Gas Industry*, vol. 33, no. 2, pp. 71–75, 2013.

[7] V. A. Dunayevsky and F. Abbassian, "Application of stability approach to bit dynamics," *SPE Drilling & Completion*, vol. 13, no. 2, pp. 99–107, 1998.

[8] P. A. Wand, M. Bible, and I. Silvester, "Risk-based reliability engineering enables improved rotary-steerable-system performance and defines new industry performance metric," in *Proceedings of the IADC/SPE Drilling Conference, SPE-98150-MS*, Society of Petroleum Engineers, Miami, FL, USA, February 2006.

[9] A. Lubinski, "A study of the buckling of rotary drilling strings," in *Proceedings of the 1950 Spring Meeting*, pp. 178–214, New York, NY, USA, March 1950.

[10] J. J. Bailey and I. Finnie, "An analytical study of drill-string vibration," *Journal of Engineering for Industry*, vol. 82, no. 2, pp. 122–127, 1960.

[11] P. R. Paslay and D. B. Bogy, "Drill string vibrations due to intermittent contact of bit teeth," *Journal of Engineering for Industry*, vol. 85, no. 2, pp. 187–194, 1963.

[12] D. W. Dareing and B. J. Livesay, "Longitudinal and angular drill-string vibrations with damping," *Journal of Engineering for Industry*, vol. 90, no. 4, pp. 671–679, 1968.

[13] K. K. Millheim and M. C. Apostal, "How BHA dynamics affect bit trajectory," *WorldOil*, vol. 92, no. 6, pp. 183–205, 1981.

[14] V. A. Dunayevsky, F. Abbassian, and A. Judzis, "Dynamic stability of drillstrings under fluctuating weight on bit," *SPE Drilling & Completion*, vol. 8, no. 2, pp. 84–92, 1993.

[15] J. D. Jansen, "Whirl and chaotic motion of stabilized drill collars," *SPE Drilling Engineering*, vol. 7, no. 2, pp. 107–114, 1992.

[16] A. H. Mizajanzade, A. I. Bulatov, A. M. Gusman, and S. A. Shirinzade, "Well drilling and cementing: a systems approach, models and artificial intelligence," in *Proceedings of the 13th World Petroleum Conference, WPC-24151*, Buenos Aires, Argentina, October 1991.

[17] M. W. Dykstra, D. C. K. Chen, T. M. Warren, and S. A. Zannoni, "Experimental evaluations of drill bit and drill string dynamics," in *Proceedings of the 1994 SPE Annual Technical Conference and Exhibition, SPE-28323-MS*, New Orleans, LA, USA, September 1994.

[18] S. Wolf, M. Zacksenhouse, and A. Arian, "Field measurements of downhole drillstring vibrations," in *Proceedings of the SPE Annual Technical Conference and Exhibition, SPE-14330-MS*, Society of Petroleum Engineers, Las Vegas, NV, USA, 1985.

[19] D. A. Close, S. C. Owens, and J. D. MacPherson, "Measurement of BHA vibration using MWD," in *Proceedings of the IADC/SPE Drilling Conference, SPE-17273-MS*, Society of Petroleum Engineers, Dallas, TX, USA, February 1998.

[20] J. D. Macpherson and P. Jogi, "Application and analysis of simultaneous near bit and surface dynamics measurements," in *Proceedings of the 1998 IADC/SPE Drilling Conference, SPE-39397-MS*, Dallas, TX, USA, March 1998.

[21] P. N. Jogi, J. D. Macpherson, and M. Neubert, "Field verification of model-derived natural frequencies of a drill string," *Journal of Energy Resources Technology*, vol. 124, no. 3, pp. 154–162, 2002.

[22] A. S. Yigit and A. P. Christoforou, "Stick-slip and bit-bounce interaction in oil-well drillstrings," *Journal of Energy Resources Technology*, vol. 128, no. 4, pp. 268–274, 2006.

[23] L. W. Ledgerwood III, J. R. Jain, O. J. Hoffmann, and R. W. Spencer, "Downhole measurement and monitoring lead to an enhanced understanding of drilling vibrations and polycrystalline diamond compact bit damage," *SPE Drilling and Completion*, vol. 28, no. 3, pp. 254–262, 2013.

[24] H. Oueslati, A. Hohl, N. Makkar, T. Schwefe, and C. Herbig, "The need for high frequency vibration measurement along with dynamics modeling to understand the genesis of PDC bit damage," in *Proceedings of the 2014 IADC/SPE Drilling Conference and Exhibition, SPE-167993-MS*, Society of Petroleum, Fort Worth, TX, USA, March 2014.

[25] T. Baumgartner and E. van Oort, "Pure and coupled drill string vibration pattern recognition in high frequency

downhole data," in *Proceedings of the SPE Annual Technical Conference and Exhibition, SPE-170955-MS*, Society of Petroleum Engineers, Amsterdam, Netherlands, October 2014.

[26] G. Liu, Z. Jia, Z. Liu, and B. He, "Sand content monitoring method of heave oil wells based on high-frequency vibration signal analysis," *Journal of China University of Petroleum*, vol. 35, no. 3, pp. 84–88, 2011.

[27] A. Arnaout, P. Zoellner, G. Thonhauser, and N. Johnstone, "Intelligent data quality control of real-time rig data," in *Proceedings of the SPE Middle East Intelligent Energy Conference and Exhibition, SPE-167437-MS*, Society of Petroleum Engineers, Manama, Bahrain, October 2013.

[28] W. Liu, D. Tao, H. Miao et al., "Structural design of linear drilling shale shaker," *Mechanical engineering and automation*, vol. 2014, no. 3, pp. 102–104, 2014.

[29] G. Liu, Q. Yang, Z. Dong, B. He, and Z. Geng, "A drill bit vibration anti-collision monitoring system and field experiment," *Natural Gas Industry*, vol. 33, no. 6, pp. 66–70, 2013.

[30] G. Dong and P. Chen, "A review of the evaluation, control, and application technologies for drill string vibrations and shocks in oil and gas well," *Shock and Vibration*, vol. 2016, Article ID 7418635, 34 pages, 2016.

[31] J. Sugiura and S. Jones, "A drill bit and drilling motor with embedded high-frequency 1600 Hz drilling dynamics sensors provide new insights into challenging downhole drilling conditions," in *Proceedings of the SPE/IADC International Drilling Conference and Exhibition, SPE-194138-MS*, Society of Petroleum Engineers, Hague, Netherlands, March 2019.

[32] H. Nyquist, "Certain topics in telegraph transmission theory," *Transactions of the American Institute of Electrical Engineers*, vol. 47, no. 2, pp. 617–644, 1928.

[33] S. A. Zannoni, C. A. Cheatham, D. C. K. Chen, and C. A. Golla, "Development and field testing of a new downhole MWD drillstring dynamics sensor," in *Proceedings of the SPE Annual Technical Conference and Exhibition*, SPE-26341-MS, Houston, TX, USA, October 1993.

[34] G. Heisig, J. Sancho, and J. D. Macpherson, "Downhole diagnosis of drilling dynamics data provides new level drilling process control to driller," in *Proceedings of the SPE Annual Technical Conference and Exhibition, SPE-49206-MS*, Society of Petroleum Engineers, New Orleans, LA, USA, January 1998.

[35] J. T. Finger, A. J. Mansure, S. D. Knudsen, and R. D. Jacobson, "Development of a system for diagnostic-while-drilling (DWD)," in *Proceedings of the SPE/IADC Drilling Conference, SPE-79884-MS*, Society of Petroleum Engineers, Amsterdam, Netherlands, February 2003.

[36] S. L. Chen, K. Blackwood, and E. Lamine, "Field investigation of the effects of stick-slip, lateral, and whirl vibrations on rollercone bit performance," *SPE Drilling and Completion*, vol. 17, no. 1, pp. 15–20, 2002.

[37] J. Greenberg, "Weatherford sensors track vibration to increase ROP, temperature change for early kick detection," *Drilling Contractor*, vol. 64, no. 2, pp. 46-47, 2008.

[38] W. G. Lesso, M. Ignova, F. Zeineddine, J. M. Burks, and J. B. Welch, "Testing the combination of high frequency surface and downhole drilling mechanics and dynamics data under a variety of drilling conditions," in *Proceedings of the SPE/IADC Drilling Conference and Exhibition, SPE-140347-MS*, Society of Petroleum Engineers, Amsterdam, Netherlands, January 2011.

[39] P. D. Ambrosio, R. Bouska, A. J. Clarke, J. L. Laird, J. E. Mckay, and S. T. Edwards, "Distributed dynamics feasibility study," in *Proceedings of the IADC/SPE Drilling Conference and Exhibition, SPE-151477-MS*, Society of Petroleum Engineers, San Diego, CA, USA, March 2012.

[40] N. Cardy, F. Hjortland, C. Jeffrey, S. Wilde, N. Muecke, and A. Wroth, "Along string dynamics measurements reveal isolated potentially damaging upper string vibration environments," in *Proceedings of the IADC/SPE Drilling Conference and Exhibition, SPE-178872-MS*, Society of Petroleum Engineers, Fort Worth, TX, USA, March 2016.

[41] H. Oueslati, J. R. Jain, H. Reckmann, L. W. Ledgerwood, R. Pessier, and S. Chandrasekaran, "New insights into drilling dynamics through high-frequency vibration measurement and modeling," in *Proceedings of the SPE Annual Technical Conference and Exhibition, SPE-166212-MS*, Society of Petroleum Engineers, New Orleans, LA, USA, October 2013.

[42] O. J. Hoffmann, J. R. Jain, R. W. Spencer, and N. Makkar, "Drilling dynamics measurements at the drill bit to address today's challenges," in *Proceedings of the 2012 Instrumentation & Measurement Technology Conference*, pp. 1–6, IEEE, Graz, Austria, July 2012.

[43] Y. Wang, Y. Shen, M. Charter, and G. Skoff, "High frequency vibration measurement coupled with time-based dynamic simulations: new system to predict/solve instability issues," in *Proceedings of the SPE Annual Technical Conference and Exhibition, SPE-170708-MS*, Society of Petroleum Engineers, Amsterdam, Netherlands, October 2014.

[44] Z. Zhang, Y. Shen, W. Chen et al., "Continuous high frequency measurement improves understanding of high frequency torsional oscillation in north America land drilling," in *Proceedings of the SPE Annual Technical Conference and Exhibition, SPE-187173-MS*, Society of Petroleum Engineers, San Antonio, TX, USA, October 2017.

[45] "BlackStream 6.75-in. EMS downhole measurement tool, CMKT-5319_ENG_v02," 2018, https://www.nov.com/.

[46] "4-in. BlackStream ASM dynamics tool, tool specification, NOV-DDS-TS-1391-001," 2016, https://www.nov.com/.

[47] "5 in. BlackStream MWD tool, tool specification, NOV-DDS-TS-0000-000," 2020, https://www.nov.com/.

[48] CuBIC® HF, *High-Frequency Drilling Dynamics Recorder*, Sanvean Technologies, Turbo Drill Industries Inc., Conroe, TX, USA, 2019, https://www.sanveantech.com/.

[49] H. Kong, K. Lan, X. Liu, M. Liu, W. Chao, and L. Xi, "Analysis of and countermeasure for bit failures in heterogeneous strata based on vibration measurement," *Natural Gas Industry*, vol. 39, no. 12, pp. 110–115, 2019.

[50] "BlackBox eclipse II downhole measurement tool, tool specification, JIRA 11299," 2020, https://www.nov.com/.

[51] A. Bowler, R. Harmer, L. Logesparan, J. Sugiura, B. Jeffryes, and M. Ignova, "Continuous high-frequency measurements of the drilling process provide new insights into drilling-system response and transitions between vibration modes," in *Proceedings of the SPE Annual Technical Conference and Exhibition, SPE-170713-MS*, Society of Petroleum Engineers, Amsterdam, Netherlands, October 2014.

[52] W. Emmerich, A. Greten, I. B. Brahim, and O. Akimov, "Evolution in reliability of high-speed mud pulse telemetry," in *Proceedings of the Offshore Technology Conference, OTC-26886-MS*, Houston, TX, USA, 2016.

[53] C. Carpenter, "Wired-drillpipe technology in a deep ultra-depleted reservoir," *Journal of Petroleum Technology*, vol. 66, no. 6, pp. 101–103, 2014.

[54] A. D. Craig, T. A. Jackson, D. Ramnarace, R. Schultze, and M. Briscoe, "The evolution of wired drilling tools: a background, history and learnings from the development of a suite of drilling yools for wired drillstrings," in *Proceedings of the*

SPE/IADC Drilling Conference, SPE-163416-MS, Society of Petroleum Engineers, Amsterdam, Netherlands, March 2013.

[55] D. Denney, "Distributed-dynamics feasibility study," *Journal of Petroleum Technology*, vol. 65, no. 2, pp. 100–107, 2013.

[56] O. Akimov, A. Hohl, H. Oueslati, and H. Reckmann, "Evolution of drilling dynamics measurement systems," in *Proceedings of the SPE/IADC Middle East Drilling Technology Conference and Exhibition, SPE-189431-MS*, Society of Petroleum Engineers, Abu Dhabi, UAE, January 2018.

[57] N. Al-Shuker, C. Kirby, and M. Brinsdon, "The application of real time downhole drilling dynamic signatures as a possible early indicator of lithology changes," in *Proceedings of the SPE/DGS Saudi Arabia Section Technical Symposium and Exhibition, SPE-149056-MS*, Society of Petroleum Engineers, Al-Khobar, Saudi Arabia, May 2011.

[58] R. Gee, C. Hanley, R. Hussain, L. Canuel, and J. Martinez, "Axial oscillation tools vs. lateral vibration tools for friction reduction—what's the best way to shake the pipe?" in *Proceedings of the SPE/IADC Drilling Conference and Exhibition, SPE-173024-MS*, Society of Petroleum Engineers, London, UK, March 2015.

[59] R. J. Shor, M. W. Dykstra, O. J. Hoffmann, and M. Coming, "For better or worse: applications of the transfer matrix approach for analyzing axial and torsional vibration," in *Proceedings of the SPE/IADC Drilling Conference and Exhibition, SPE-173121-MS*, Society of Petroleum Engineers, London, UK, March 2015.

[60] S. Jones, C. Feddema, J. Sugiura, and J. Lightey, "A new friction reduction tool with axial oscillation increases drilling performance: field-testing with multiple vibration sensors in one drill string," in *Proceedings of the IADC/SPE Drilling Conference and Exhibition, SPE-178792-MS*, Society of Petroleum Engineers, Fort Worth, TX, USA, March 2016.

[61] P. A. Patil and O. N. Ochoa, "Identification of optimal drilling parameters for reduction of high-frequency torsional oscillations by combined approach with modeling and real-time analysis of high-frequency measurements," in *Proceedings of the IADC/SPE International Drilling Conference and Exhibition, SPE-199680-MS*, Society of Petroleum Engineers, Galveston, TX, USA, March 2020.

[62] Y. Shen, W. Chen, Z. Zhang et al., "Drilling dynamics model to mitigate high frequency torsional oscillation," in *Proceedings of the IADC/SPE International Drilling Conference and Exhibition, SPE-199634-MS*, Society of Petroleum Engineers, Galveston, TX, USA, March 2020.

[63] J. K. Wilson, "Field validation of a new bottomhole-assembly model for unconventional shale plays," *SPE Drilling & Completion*, vol. 34, no. 2, pp. 189–206, 2019.

[64] T. M. Warren and J. H. Oster, "Torsional resonance of drill collars with PDC bits in hard rock," *Journal of Petroleum Technology*, vol. 51, no. 2, pp. 625–637, 1999.

[65] P. E. Pastusek, E. Sullivan, and T. M. Harris, "Development and utilization of a bit based data acquisition system in hard rock PDC applications," in *Proceedings of the SPE/IADC Drilling Conference, SPE-105017-MS*, Society of Petroleum Engineers, Amsterdam, Netherlands, February 2007.

[66] L. A. Lines, D. R. H. Stroud, and V. A. Coveney, "Torsional resonance—an understanding based on field and laboratory tests with latest generation point-the-bit rotary steerable system," in *Proceedings of the SPE/IADC Drilling Conference, SPE-163428-MS*, Society of Petroleum Engineers, Amsterdam, Netherlands, March 2013.

[67] V. S. Tikhonov and O. S. Bukashkina, "A new model of high-frequency torsional oscillations (HFTO) of drillstring in 3-D wells," in *Proceedings of the International Petroleum Technology Conference, IPTC-17958-MS*, Kuala Lumpur, Malaysia, December 2014.

[68] A. Hohl, M. Tergeist, H. Oueslati et al., "Derivation and experimental validation of an analytical criterion for the identification of self-excited modes in drilling systems," *Journal of Sound and Vibration*, vol. 2015, no. 2, pp. 1–13, 2015.

[69] A. Hohl, M. Tergeist, H. Oueslati et al., "Prediction and mitigation of torsional vibrations in drilling systems," in *Proceedings of the IADC/SPE Drilling Conference and Exhibition, SPE-178874-MS*, Society of Petroleum Engineers, Fort Worth, TX, USA, March 2016.

[70] A. Hohl, E. Palata, and P. Arevalo, "Real-time system to calculate the maximum load of high-frequency torsional oscillations independent of sensor positioning," in *Proceedings of the SPE/IADC International Drilling Conference and Exhibition, SPE-194071-MS*, Society of Petroleum Engineers, Hague, Netherlands, March 2019.

[71] J. Sugiure and S. Jones, "Simulation and measurement of high-frequency torsional oscillation HFTO/high-frequency axial oscillation HFAO and downhole HFTO mitigation: knowledge gains continue by using embedded high-frequency drilling dynamics sensors," in *Proceedings of the IADC/SPE International Drilling Conference and Exhibition, SPE-199658-MS*, Society of Petroleum Engineers, Galveston, TX, USA, March 2020.

[72] L. Lines, "Technology update: a holistic approach to controlling torsional dynamics in the drillstring," *Journal of Petroleum Technology*, vol. 68, no. 10, pp. 20–23, 2016.

[73] A. Hohl, V. Kulke, A. Kueck, C. Herbig, H. Reckmann, and G. Ostermeyer, "The nature of the interaction between stick/slip and high-frequency torsional oscillations," in *Proceedings of the IADC/SPE International Drilling Conference and Exhibition, SPE-199642-MS*, Society of Petroleum Engineers, Galveston, TX, USA, March 2020.

[74] J. R. Jain, H. Oueslati, A. Hohl et al., "High-frequency torsional dynamics of drilling systems: an analysis of the bit-system interaction," in *Proceedings of the IADC/SPE Drilling Conference and Exhibition, SPE-167968-MS*, Society of Petroleum Engineers, Fort Worth, TX, USA, March 2014.

[75] D. Heinisch, V. Kulke, V. Peters et al., "Simulation and testing of an isolator tool for high-frequency torsional oscillation," in *Proceedings of the Abu Dhabi International Petroleum Exhibition and Conference, SPE-193313-MS*, Society of Petroleum Engineers, Abu Dhabi, UAE, November 2018.

[76] C. Carpenter, "Isolator tool for high-frequency torsional oscillation proves effective," *Journal of Petroleum Technology*, vol. 71, no. 12, pp. 64-65, 2019.

[77] G. Xie and X. Zhou, "Theoretical analysis and practice of high frequency digital signal while drilling in petroleum engineering," *Journal of Wuzhou University*, vol. 3, no. 18, pp. 25–30, 2008.